School of Engineering
Howard University

STUDY OF FOLDABLE ELASTIC TUBES for LARGE SPACE STRUCTURE APPLICATIONS

Final Report

for

Phase I

by
Irving W. Jones
Collins Boateng
Caster D. Williams
January 1980

Conducted under NASA Grant NSG 1320

Principal Investigator

Irving W. Jones, Ph.D.
Professor, Civil Engineering
Howard University

NASA Technical Officer:

Garnett C. Horner, Ph.D.
Structural Mechanics Engineer
Langley Research Center

PREFACE

The research reported here was conducted at Howard University under NASA Grant NSG 1320: Graduate Research Program in Advanced Aerospace Structures.

Supervisor for the project was Dr. Irving W. Jones. The work has been monitored by Dr. G. C. Horner and Dr. M. F. Card of Langley. Assisting in the work were graduate research assistants Collins Boateng and Caster D. Williams, and undergraduate assistant Steve O. Mitchell. Collins Boateng has completed requirements for the masters degree under financial sponsorship of this grant. Caster Williams is due to graduate in May 1980 with the masters degree, and Steve Mitchell, a former NASA summer intern is due to graduate at the same time with the bachelors degree. He has been accepted for graduate study at Howard.

The laboratory work was performed under direct supervision of Mr. William B. Steward, who also did the drafting and some design work on the testing machine. The several vendors who provided materials and services are named in various sections of the report.

ABSTRACT

The concept of a self-deploying space structure that, after being packaged on the ground, utilizes released strain energy to accomplish deployment in space has been studied for several years. The present investigation is focusing on types of structural members that might be suitable for strain energy deployable structures, particularly for large space structure applications. Phase I, reported here, specifically examines a thin-walled cylindrical tube with a cross-section that is called "bi-convex."

The report details the design of bi-convex tube test specimens and their fabrication, the design and construction of a special purpose testing machine to test the deployment characteristics, the first series of tests and an analysis of the results.

All of the tasks leading up to the testing were accomplished with generally satisfactory results. The results of the first series of tests were quite mixed, but one clear conclusion they revealed was that since most of the specimens failed to deploy completely, due to a buckling problem, thus verifying the finding of a previous study, this type of tube requires some modification in order to be viable. Based on experience gained in this early testing, the authors have conceived several possible remedies for the buckling problem and have in fact demonstrated the effectiveness of one such modification. Optimal design of the bi-convex tube while keeping it reliable in deployment will be the aim of future work on this project.

TABLE OF CONTENTS

LIST OF FIGURES

LIST OF TABLES

1. INTRODUCTION

1.1 Background

Among the various concepts being considered by NASA for placing large trusses in space is that of collapsing a truss, or a section of one, into a compact mass while on the ground, by folding the truss members at their hinged joints and simultaneously folding certain members at their centers, the combination of folds devised to collapse the truss and thus reduce its volume to a minimum. Once in space, the packaged structure is then unfolded (or deployed) to its original configuration.

One means of accomplishing the deployment without the use of external energy is by utilizing truss members that remain elastic when folded. Such a member will release strain energy as it is unfolding, and the total structure is therefore self-deploying.

One type of member which was selected as a candidate for this function is that shown in Fig. 1.1, referred to in ref. 6 and in this report as a "bi-convex folding elastic tube" (BFET). This type of tube was first developed and studied at NASA Lewis Research Center in the mid-1960's and reported in NASA TMX 1137, ref. 1. It is described also in the patent, reference 2. At least one later patent has been granted for a revised or generalized version; that was to TRW in 1971. There, the tube was claimed to be reelable as well as foldable. In the original NASA study, the tube was envisioned primarily as a foldable fluid conduit for space applications; its potential as a structural

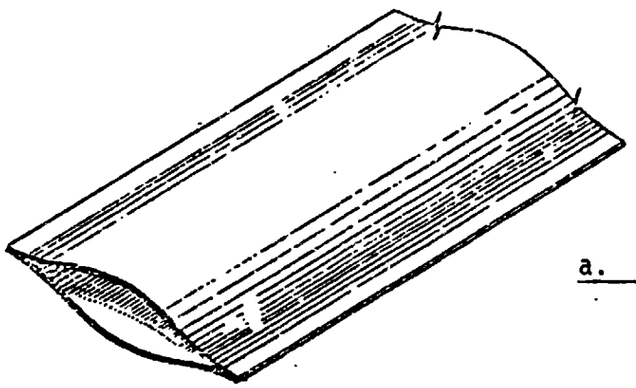

a. Section of BFET

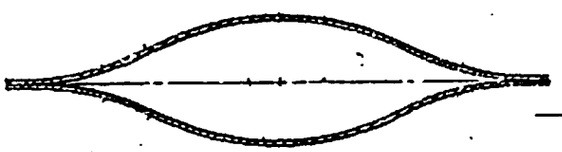

b. Tube Cross-section

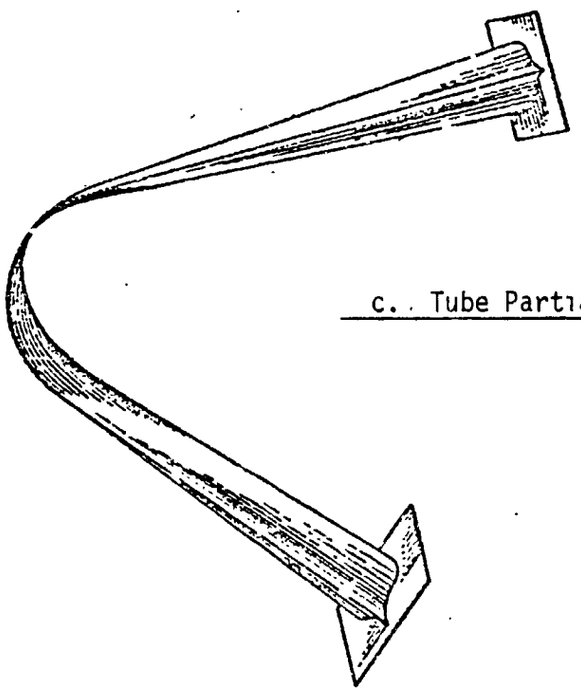

c. Tube Partially Folded

Fig. 1.1 Bi-Convex Foldable Elastic Tube

member was recognized and mentioned briefly, however. Since then it has been employed as a roll-out antenna on the Viking spacecraft and in one or two other space applications. The BFET was also the subject of comprehensive study conducted for the European Space Research Organization (ESRO) during the period 1965-1973, (ref. 3) There, a serious shortcoming in its structural behavior was repor (The present study verifies this as is discussed late

With the emergence of the LASS technology develo ment effort, interest in the bi-convex foldable elastic tube as a structural member has increased. A number of scale-model plastic space trusses, utilizing BFET's for truss members, have been fabricated and tested. Development efforts are still needed in the area of design, fabrication and testing of full-scale tubes and trusses made of the actual materials used in space structures. The present study is intended as a contribution in this problem area.

1.2 Scope and Objectives

Since this study is focused on application of the BFET concept to large space structures, the areas of interest include optimal design of members, material selection, fabrication, foldability and structural behavior. It is assumed that the BFET may be used either as the entire structural member or in the form of a hinge in the central region of a member of some other type. The test specimen geometry for this project was established with this in mind, as discussed in section 3. Up to the present time, the study has been limited to one material: stainless

steel. The unfolding tests were designed to measure or evaluate the following characteristics: foldability (will the specimen fold completely and compactly, while remaining elastic and structurally sound, then unfold completely) resisting moment versus angle during unfolding, strain energy released, compactness of the fold and transition length, i.e., length of tube that is flattened. Specimens were tested sequentially starting with the flattest shape and proceeding to the near circular. The NASA study (ref. 1) showed that a very flat shape folded easily; however it is the rounder shapes that are more efficient as columns, so that one objective here was to associate roundness with foldability and to estimate a limiting range on the cross section parameters.

2. MATERIAL SELECTION

2.1 Required Properties

The utility of the foldable elastic tube depends upon its remaining elastic throughout when it is completely collapsed. Therefore, materials with high yield strain are necessary. Yield strain is heightened by a high yield strength and/or a low modulus of elasticity. Also, fabrication and strength-to-weight considerations dictate that the material have adequate formability, weldability (or suitability to some fastening method) and low density. These requirements are met by a number of stainless steels. Also, titanium, some hard copper alloys and composites are suitable. The scope of the present study does not include a comparison of various materials or establishment of the feasibility of their use. One material,

a stainless steel was selected for use due to its relative ease of fabrication, availability, and mechanical properties.

2.2 Properties of the Selected Material

After a study of many available stainlesses, Armco 17-7PH (a semi-austenitic Armco proprietary grade) was selected for use in the initial part of this work. Armco 17-7PH is a precipitation-hardening chromium (17%) nickel (7%) stainless steel that provides, among other properties, high strength and hardness and minimum distortion on standard heat treatment. It is easily formed in the annealed condition, then may be hardened to high strength levels by heat treatments to conditions RH 950 and TH 1050 (See Appendix A). Condition TH 1050 was selected because it requires a simpler process and appeared to give satisfactory yield strength for the present application, on the basis of expected maximum stresses. However, it is noted in the product literature that full strength may not be developed when cold-worked material is heat-treated to Condition TH 1050. An alternate, but more complex heat treatment is given for this case.

Fabrication practices for 17-7PH are the same as for other chromium-nickel stainless steels.

Typical mechanical properties at room temperature are given in Table 2.1; below these in Table 2.2 are properties taken from the test report on material that was procured for the initial part of this study. The higher strength of the procured material is apparently due to its being re-rolled to thickness of 0.010" (0.25 mm). The material was procured from Rodney Teledyne Metals Company of California.

TABLE 2.1

ARMCO 17-7PH

MECHANICAL PROPERTIES, ROOM TEMPERATURE

Typical Properties[4]

Conditions	Ultimate Tensile Strength, psi (Mpa)	0.2% Tensile Yield Strength, psi (Mpa)	Elongation % in 2" (50 mm)	Hardness, Rockwell
A	130,000 (896)	40,000 (276)	35	B85
TH1050	200,000 (1379)	185,000 (1276)	9	C43
RH950	235,000 (1620)	220,000 (1517)	6	C48

TABLE 2.2

PROPERTIES OF MATERIAL FOR THIS STUDY

Conditions	Ultimate Tensile Strength, psi (Mpa)	0.2% Tensile Yield Strength, psi (Mpa)	Elongation % in 2" (50 mm)	Hardness, Rockwell
A	Longitudinal:			
	146,000 (1006)	54,000 (372)	31	B75
	Transverse:			
	146,00 (1006)	53,000 (365)	28	B75

3. DESIGN OF SPECIMENS

3.1 Assumptions

The objective in establishing the test specimen geometries was to have them proportioned to represent full-scale LASS truss members, as they are envisioned to be according to studies made to date. Since there are no established design criteria for BFET's, the procedure followed was to utilize design formulas for minimum weight circular cylindrical tubes to establish a reasonable range of radii for the given wall thickness (0.010"), and then to create a set of BFET cross-sections that would have roughly the same strength and stiffness.

3.2 "Minimum Weight" Bi-convex Tubular Columns

Previous NASA work on optimum circular column designs for large tetrahedral truss structures (ref. 5) was utilized, and the radii for a set of circular tubes designed for a loading parameter range of $2 \times 10^{-4} < P/\ell^2 < 10^{-1}$, and a length of 15 feet (both values indicated in ref. 5 to be within reason) were calculated. Also calculated were the slenderness ratios and two buckling moment values: M_b, the moment causing local buckling, according to the standard circular cylinder formula, ($\sigma_b = C_1 Et/R$, with $C_1 = 0.36$), and M_c, the maximum moment the column can take after total collapse, and still remain elastic; i.e., yield stress times section modulus of the totally flattened section. The results of these calculations are shown in the table and are plotted on Fig. 3.1

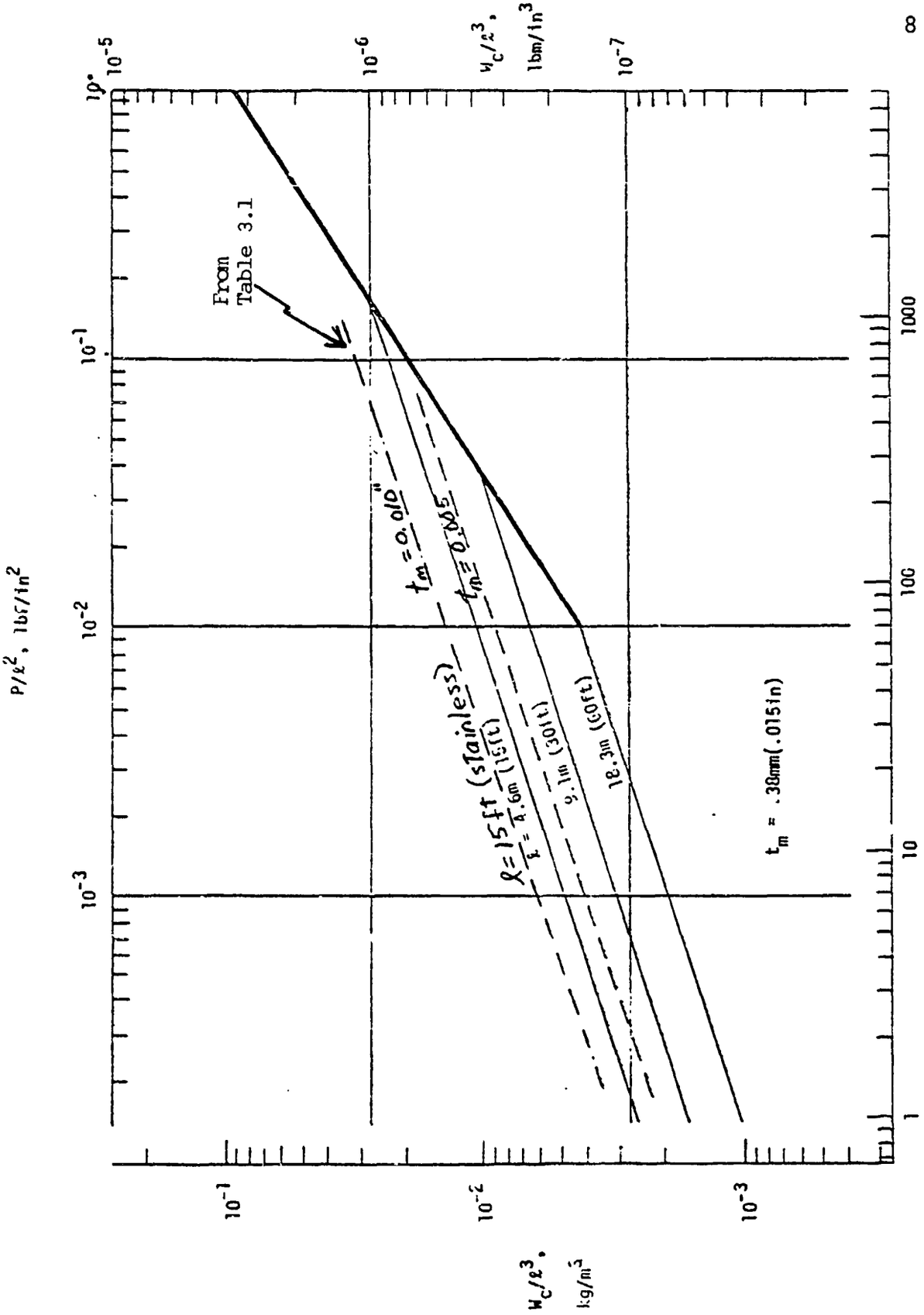

FIGURE 3.1- Weight of Thin-walled Tubular Columns
(Excerpt from Ref. 5)

TABLE 3.1

MINIMUM WEIGHT CIRCULAR TUBULAR COLUMNS

Length ℓ = 15', Minimum gage t_m = 0.010

$\frac{P}{\ell^2}$	P, lbs f	W_c, lbs m	W_c, lbs m	t, in.	R, in.	Slenderness Ratio	M_b, ft-lbs	M_c, ft-lbs
2×10^{-4}	6.5	0.093	0.95	0.010	0.29	878	82	0.38
5×10^{-4}	16.5		1.28	0.010	0.40	636	113	0.52
10^{-3}	32.4		1.61	0.010	0.50	509	141	0.65
10^{-2}	324		3.47	0.010	1.07	2 38	302	1.40
3×10^{-2}	972		5.00	0.010	1.55	164	438	2.03
5×10^{-2}	1620		5.93	0.010	1.83	139	517	2.40
10^{-1}	3240		7.47	0.010	2.31	110	653	3.02

Examination of the radii, slenderness ratios, and local buckling and collapse moments in Table 3.1 indicates that the range of radii values 1.0" < R < 2.0" appears reasonable as representative columns for this study. Since these values refer to circular columns, the next task was to determine the cross-sectional proportions of roughly equivalent BFET's.

TABLE 3.2

BFET CROSS-SECTION PARAMETERS

Inscribed Circle Radius R_3, in.	CENTRAL RADIUS R_1, in.				
1.00	1.00	1.33	(1.50)	(2.00)	(3.00)
1.50	(1.50)	(2.00)	2.25	(3.00)	4.50
2.00	(2.00)	2.67	(3.00)	4.00	6.00
	$f = \lambda/R_1$ = FLATNESS PARAMETER				
	0	0.25	0.33	0.50	0.67
	ROUND	MODERATE		FLAT	

The cross-section shape of the BFET can be defined uniquely by any three parameters (see Fig. 3.2), chosen here as R_1, the radius of the central section; R_2, the radius of the outer arcs; and f, a flatness parameter equal to λ/R_1, where λ is the distance from the neutral axis to the center of the central arc. The value f can vary from 0 to 1 in going from round to perfectly flat shapes. To determine the test specimen proportions, we start with circular cylinder radii of 1, 1.5 on 2 inches (See Table 3.2). About each of these circles we circumscribe shapes with various values of f, the flatness, and

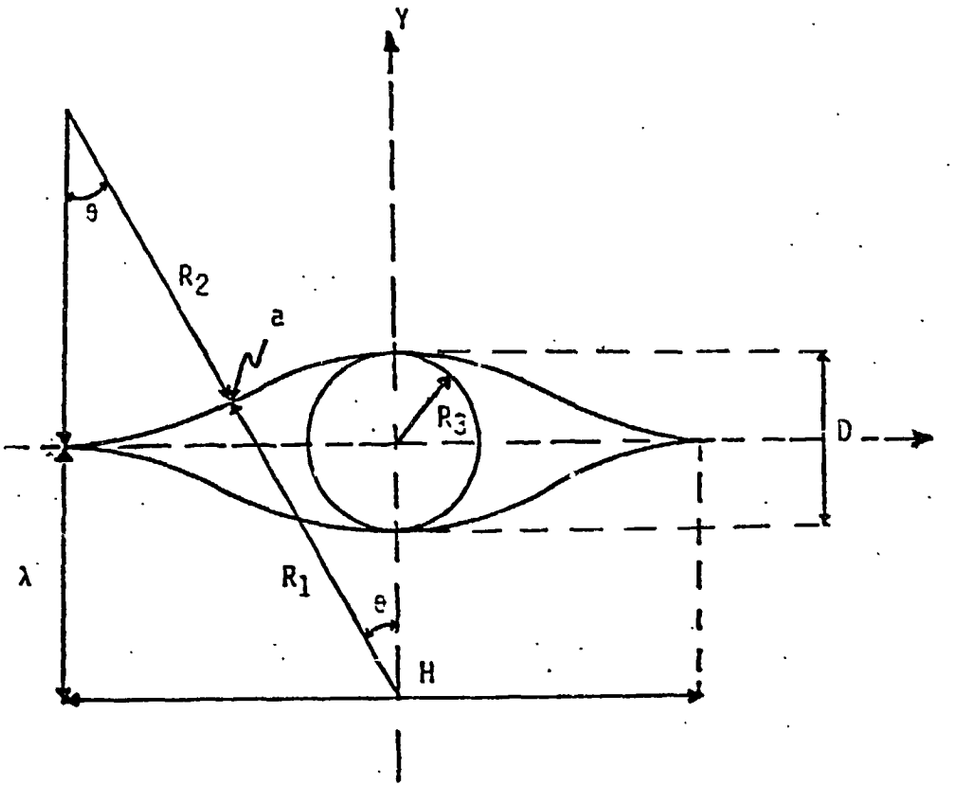

Independent cross-section parameters are:

R_1 = radius of convex segment
R_2 = radius of concave segment
λ = distance from mid-plane to center of curvature for R_1

Additional parameters are:

R_3 = radius of the inscribed circular cylinder
θ = angle to point of tangency
H = overall width
D = overall depth

Fig. 3.2 Cross-section Parameters

calculate for each the value of R_1. Out of the matrix of shapes, eight were chosen; those shown in parentheses. These particular eight were selected because their central arc radii fell in the workable range of 1.5 to 3 inches. Proceeding from the flatter to rounder tubes, would be going from left to right in Table 3.2. Three ranges: flat, moderate and round were defined as shown. The parameter that remains to be determined is the radius of the outer arcs, R_2. The arcs formed by R_2 contribute relatively little to the bending stiffness of the cross-section and therefore these arcs should ideally be kept to a minimum. However, it is clear that if they are made too small, yielding and/or stress concentrations will occur in the outer regions. The ratio R_2/R_1 should therefore be a parameter for the study. Accordingly, from each of the eight cross-sections represented by the values in parenthesis in Table 3.2 will result two specimens with R_2/R_1 equal to one, and one-half respectively.

3.3 Summary of Selected Column Geometries

The total number of specimens is sixteen. Due to cost only the first eight specimens were fabricated at this time: a, b, e, f, g, k, ℓ and m. All have $R_2 = R_1$. Properties of all specimens are summarized in Table 3.3.

3.4 Specimen Lengths

There is no clear-cut basis for determining a satisfactory length for the specimens but study of refs. 1, 3 and 6 indicates that four feet should be a sufficient length for the tubes of this study.

TABLE 3.3

TEST SPECIMEN DATA

Specimen	R_1 in.	R_2 in.	R_3 in.	λ/R_1	H in.	D in.	S	M_b in-lbs	M_c in-lbs
a	1.5	1.5	1.5	0	5.20	3	6.28	177	2.5
b	1.5	1.5	1	0.33	4.47	2	5.05	118	2.0
c	1.5	0.75	1	0.33	3.74	2	4.12	118	1.5
d	1.5	0.75	1.5	0	4.24	3	5.14	177	1.7
e	2	2	2	0	6.93	4	8.38	234	3.4
f	2	2	1.5	0.25	6.24	3	7.17	177	2.9
g	2	2	1	0.50	5.29	2	5.78	118	2.3
h	2	1	1	0.50	4.47	2	0.05	118	2.0
i	2	1	1.5	0.25	5.20	3	6.28	177	2.5
j	2	1	2	0	5.66	4	7.39	234	3.0
k	3	3	2	0.33	8.94	4	10.09	234	4.0
l	3	3	1.5	0.5	7.94	3	8.68	177	3.5
m	3	3	1	0.67	6.64	2	7.64	118	2.8
n	3	1.5	1	0.67	5.02	2	6.12	118	2.4
p	3	1.5	1.5	0.5	6.71	3	7.57	177	3.0
q	3	1.5	2	0.37	7.49	4	8.84	234	3.5

4. FABRICATION OF SPECIMENS

4.1 Preliminary

The fabrication process consisted of forming the halves of the tubes (the shells), fastening them along their edges, heat-treating and fitting them with end plates to accommodate their installation into the FET testing machine and also to accommodate installation into the compression testing machine for buckling tests to be conducted later.

Various methods were explored for forming the shells, and the advice of various manufacturing specialists was sought. The methods included deep drawing, hydraulic forming, explosive forming, cold rolling, and rubber pad forming. The latter process was selected because it was the least expensive relative to projected costs of the others, and it had been used successfully in the ESRO work (3).

4.2 Rubber Pad (Guerin) Forming Process

Rubber pad forming employs either a monolithic or layered rubber pad encased in a heavy retainer. The pad acts in the manner of the female part of a die. A form block, or punch, acts as the male part in conventional forming. The block is secured either to the ram or the platen of the press. The blank (the piece to be formed) is positioned between the form block and the rubber pad, and as the two are brought together, the blank is forced into the rubber pad and is bent into the shape of the form block. The rubber acts somewhat like a hydraulic fluid in exerting nearly equal pressure over the surface of the blank

Some advantages of this process are: (1) one pad takes the place of many die shapes, (2) the form block can be made of cheaper and easier-to-shape materials than in conventional forming (3) thinning of the work metal (such as occurs in deep drawing) is practically eliminated. Some disadvantages normally associated with the method are: (1) the rubber wears out or tears on long production runs (2) definition may be hard to obtain on pieces with sharp edges. Neither of these disadvantages was a factor in our particular application.

The forming set-up was as shown in Figure 4.1. A multi-layered rubber pad was encased in the steel retainer box. The box was supported on two steel horses which were already available in the laboratory. Above, the precisely contoured form block was secured to the 4' x 4' head plate of the 600,000 lb. capacity universal testing machine, which was utilized as the press. Each rectangular sheet, or blank, was positioned on the form block by inserting its two locating holes into the corresponding two locating pins (one at each end) on the block. The blank was lubricated with drawing wax prior to fastening. As the press was lowered, the blank was formed into the shape of the block; upon removal of the pressure, it sprang back to a shape of lesser curvature. (Theoretically, a properly calculated form block contour should produce the desired final shape.)

4.3 Form Blocks

The shapes of the form blocks were determined from an equation derived for that purpose in Appendix C of ref. 3, which expresses the radius of a circular arc into which a plane thin sheet must be bent

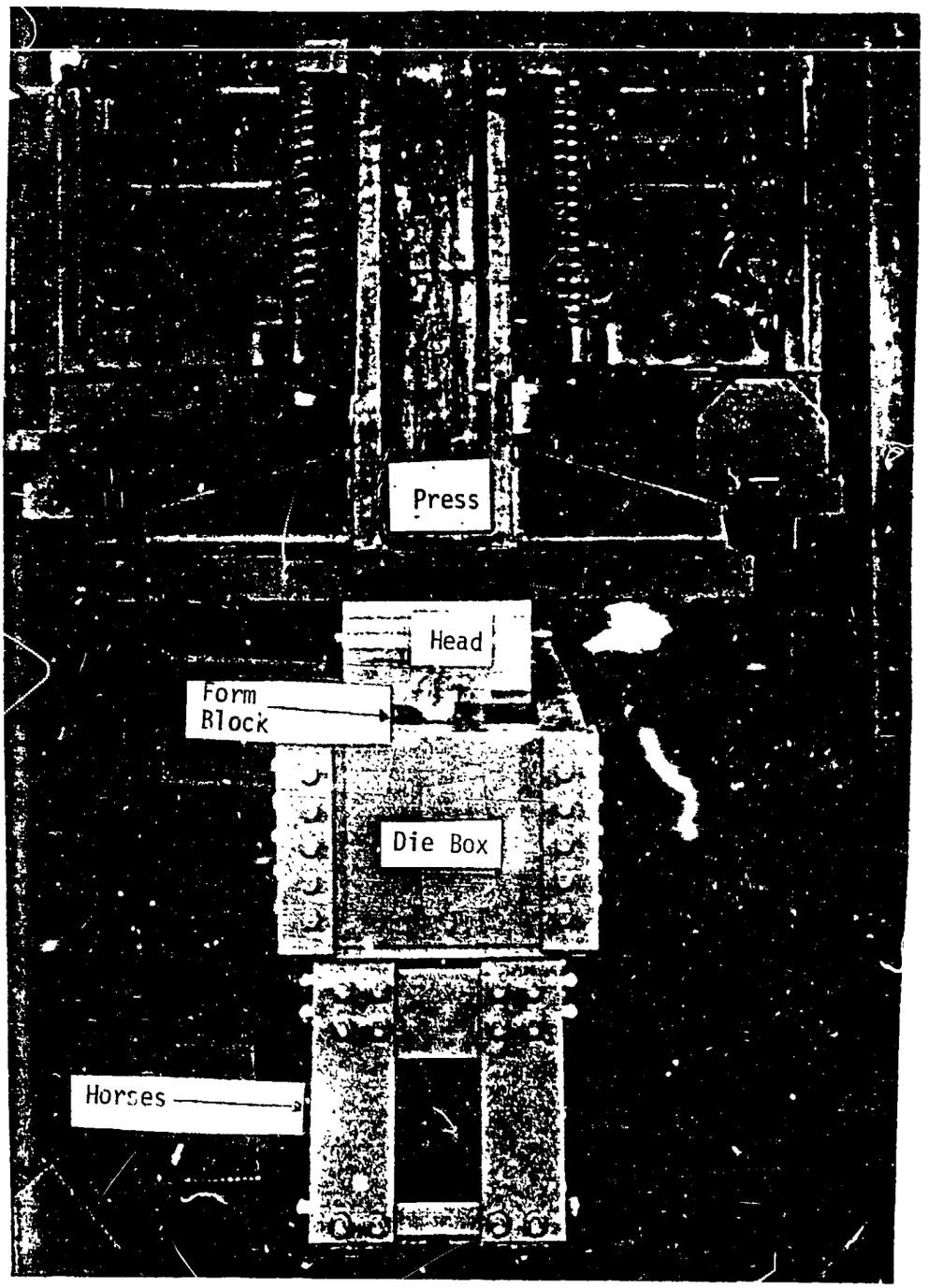

Fig. 4.1 Front View of Die Box and Form Block.

in order to have it spring back to a prescribed arc upon unloading. When loaded, the sheet is partially yielded and is assumed to behave according to Tresca's Yield Criterion. Based upon this equation and simple geometric relationships, a computer program was written to calculate and plot the form block shapes for the 16 specimens.

Based upon these shapes, detailed drawings were made for the form blocks (See Appendix B for typical shape). The blocks were made out of hardwood.

Since the blocks had to be interchanged, they were mounted into a head block (fig. 4.1) which in turn was mounted into the platen of the press.

4.4 Die Box

The die box, or retainer, is also shown in fig. 4.1. It was designed to withstand a pressing force of about 150,000 lbs. It was constructed out of A 36 structural steel and high strength A 326 3/4" diameter bolts. It consists of essentially four 15" channels (the sides) whose flanges serve to hold down the rubber when it is being pressed down at the center. Its bolted construction permits lengthening the box in the future, if desired, by adding new sections. The box was constructed by the J.B. Kendall Company, of Washington, D.C.

4.5 Rubber Pad

The rubber pad consists of 14 layers of 1/2 inch thick neoprene with a Durometer hardness of A 60, considered moderate for forming. The layers were not laminated, but adhered to each other under the

pressure, so that the pad acted as an integral mass. Overall dimensions of the pad were roughly 55" x 14" in area and 7" deep. The bottom of the retainer was filled with plywood. Experimentation led to arriving at an optimum cross-sectional shape for the pad. While some forming by this process can be done with a purely rectangular pad, in this instance it was necessary to cut away strips of material from the center region of the upper four or so layers to form a cavity roughly the shape of the form block; thus the rubber was required to do less distorting to accept the penetrating form block.

Air space had to be left in the corners to provide room for the rubber to move in. The rubber endured the forming of the 54 shells for the first series of three shapes of specimens, but in some places was beginning to wear. It was then replaced by a second pad which lasted to the completion of the eight shapes. Layers were interchanged between runs, and the cavity shape had to be adjusted with each progression to a different shape.

4.6 Blanking

The blanks were cut out of 24 inch wide rolls of sheet by the steel supplier. The 24 inch wide roll was run through a slitting machine to produce rolls with widths equal to the arc lengths of the specimens. ("S" in Table 3.3). These were then sheared off into four foot lengths. Locating holes 1/4" in diameter were punched in the blanks at each end. Small pieces were also furnished for coupon testing.

4.7 Forming Trials

Before undertaking the forming of the specimens, a small forming set-up (8½" x 9" x 10" deep box, rubber pad and 200,000 lb. press) was used to experiment with the process and gain some skill and experience with the method. Two types of rubber were tried: Pure gum (A 35 Hardness) and neoprene (A 60 Hardness). The latter was adopted for superior performance and wear.

4.8 Forming

The forming of the specimens was accomplished with the same procedure as in the trial set-up. A force of 125,000 to 150,000 lbs was applied to the system. Upon removal of the force, it was found that most of the specimens sprang back to shapes with less curvature than the calculated value, and that with a second application of the force, the curvatures increased somewhat. In the end, three of the specimens (b, g and f) had shapes close to the calculated ones and the others were somewhat flatter. This was not considered serious because they all were within the range of definitive shape values (R and f) originally established for the study, and also for each shape, the shells came out identical.

4.9 Fastening

Three possible methods of fastening the shells along their seams were considered. These were seam-welding (used by NASA, ref. 1), spot-welding (used by ESRO, ref. 3) and brazing. Brazing was at first suggested as being preferable because it could be done in the same operation with the heat-treatment in a vacuum furnace. This suggestion turned out to be virtually impossible to implement essentially because

brazing is a relatively delicate technique requiring skill and experience to achieve just the right amount and type of capillary action. With a thin material this becomes even more difficult.

After an attempt by a vendor to braze/heat-treat several specimens was unsuccessful, attention was turned to seam welding. This method of fastening was successfully accomplished by the Lavelle Aircraft Co. of Newtown, Pa. on an electric arc resistance seam-welding machine with circular electrodes. It was necessary to modify the machine to apply the unusually low pressure required for this application. The welding was done in a satisfactory manner, but in the process of handling the tubes for welding, they were inadvertantly flattened slightly.

4.10 Heat Treatment

After welding, the tubes were shipped to the Met-lab Company in Philadelphia for precipitation hardening heat treatment. The treatment sequence is discussed in section 2. After a trial run showed that the tubes tended to flatten while in the furnace, it was decided to place an insert (a stainless steel circular cylindrical pipe) inside each tube to preserve its shape. This helped, but the tubes all turned out to have flatter shapes than expected. This is discussed later in section 7.

5. FOLDING ELASTIC TUBE TESTING MACHINE

5.1 Configuration and Operation

An assembly drawing of the testing machine is shown in Appendix C and photographs in fig. 5.1. As shown, it has two arms, one fixed and one which rotates, hinged at a central vertical shaft: The arms are

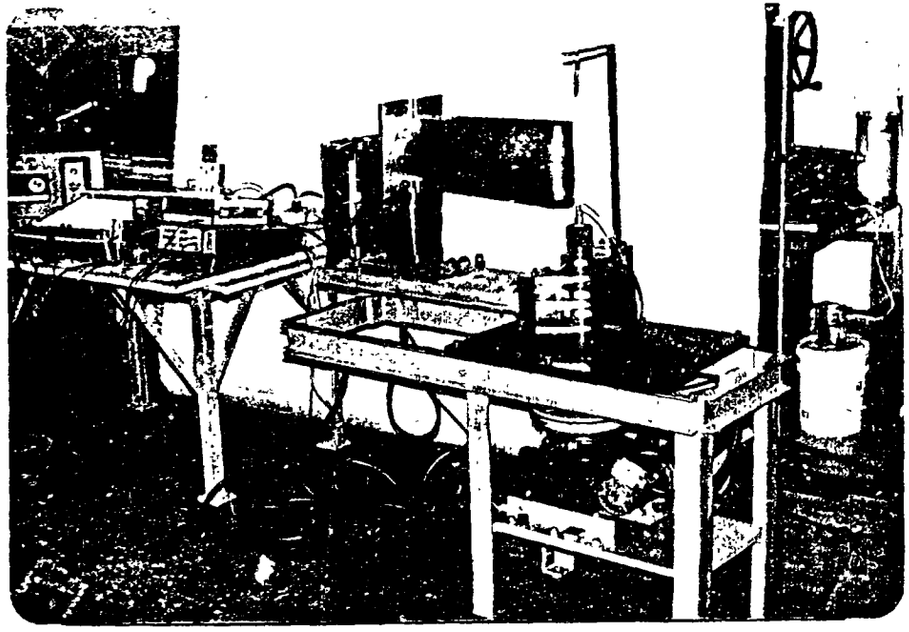

a. Folded

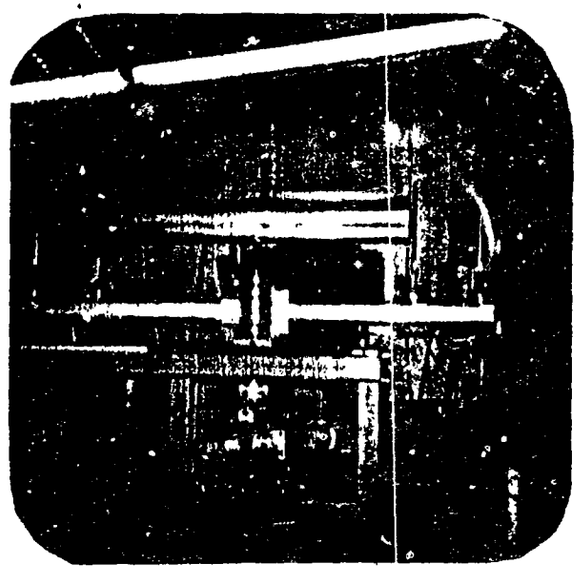

C. Fully Deployed

Fig. 5.1 FET Testing Machine in Operation

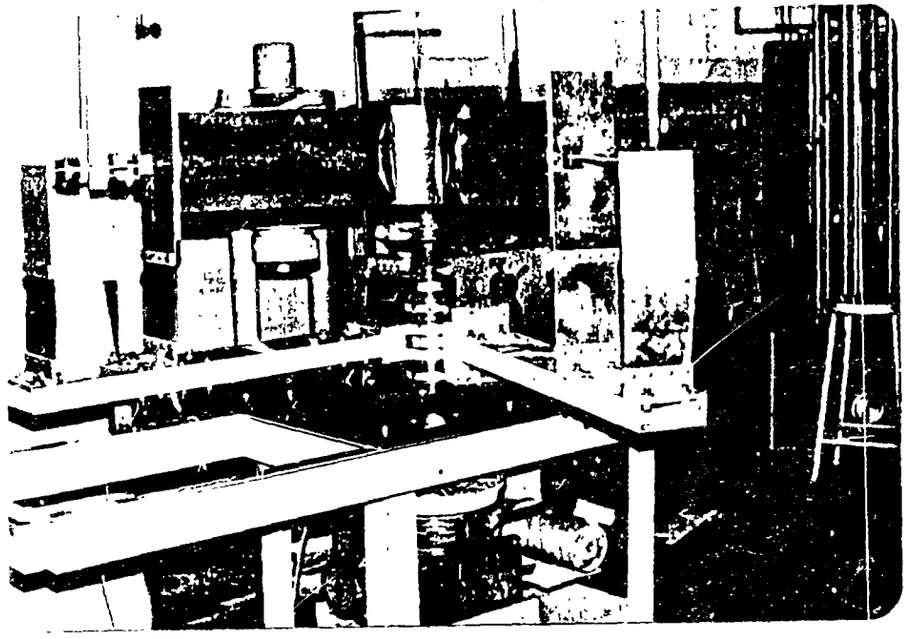

b. Partially Deployed

approximately 5-1/2 feet long each, and are made of rectangular aluminum tubing. The central fittings (hinges) are of machined aluminum and are installed in ball bearings for minimum friction. The assembly rests on a supporting stand and the arms rotate in a horizontal plane. Near the outboard end of each arm is a plate onto which the specimen end piece (insert) is attached. The flex plates permit the specimen to extend freely in the longitudinal direction. With the arms in a straight configuration, the test specimen is bolted to the plates in such a manner that it will receive a pure bending moment through its centroidal axis when the movable arm is rotated. The tube is flattened in the center region, and the arm is rotated through 180°, i.e., until it is parallel to the fixed arm. The half of the specimen attached to the rotating arm also rotates through 180° thus folding the specimen. The reaction acting against the stationary arm is picked up by a load cell mounted against it near the outboard end. The shaft of the movable arm is connected to a variable speed gear drive that was installed to regulate the rate of unfolding. A magnetic clutch mounted on the shaft permits completely free release of the specimen.

5.2 Instrumentation

As the specimen is unfolded, resisting moment is measured by a B-L-H Type Load Cell placed approximately 19" behind, and toward the outward end of the stationary arm. This load cell is connected laterally between the arm and the supporting table. The cell voltage is registered and displayed by a DORIC model 420 transducer indicator with a sensitivity of $\pm$ 0.001V. A trans-tek angular

displacement transducer simultaneously measures the angle of rotation. The signals from the load cell and the displacement transducer actuate an H-P model 7004B x-y recorder connected to the set up. The x-y recorder simultaneously proceeds to plot the M-θ curve. The entire set up is powered by an H-P model 6216 power supply. The amount of power required was fifteen volts. A diagrammatic representation of the set-up is shown in Fig. 5.2.

6. TEST PLAN

6.1 Preparation of Specimens

The centerlines of the completed specimens were marked along the lateral and longitudinal axes. Graduations at one inch intervals were marked off out to eight inches on both sides of the centerline. This permitted uniform placement of the collapsing clamps.

The specimens were identified by engraved designations giving shape (A, B, E, F, G, K, L and M) followed by 79 (the year fabricated) and a number; e.g., G-79-1, etc.

6.2 Deployment Test Procedure

The first test run on a new specimen consisted of the eight steps listed below. Steps five through eight were repeated for any subsequent tests run on the same specimen.

(1) Installation of Wood Inserts

A wood insert having the same cross-sectional shape as the tube and a thickness of 1.5 inches was pushed into each end of the tube. The insert was fastened to the tube by four screws.

(2) Attachment of End Plates

Three rectangular patterns of 4 holes each, one pattern for each depth of specimen (2, 3 and 4 inches) were drilled into the

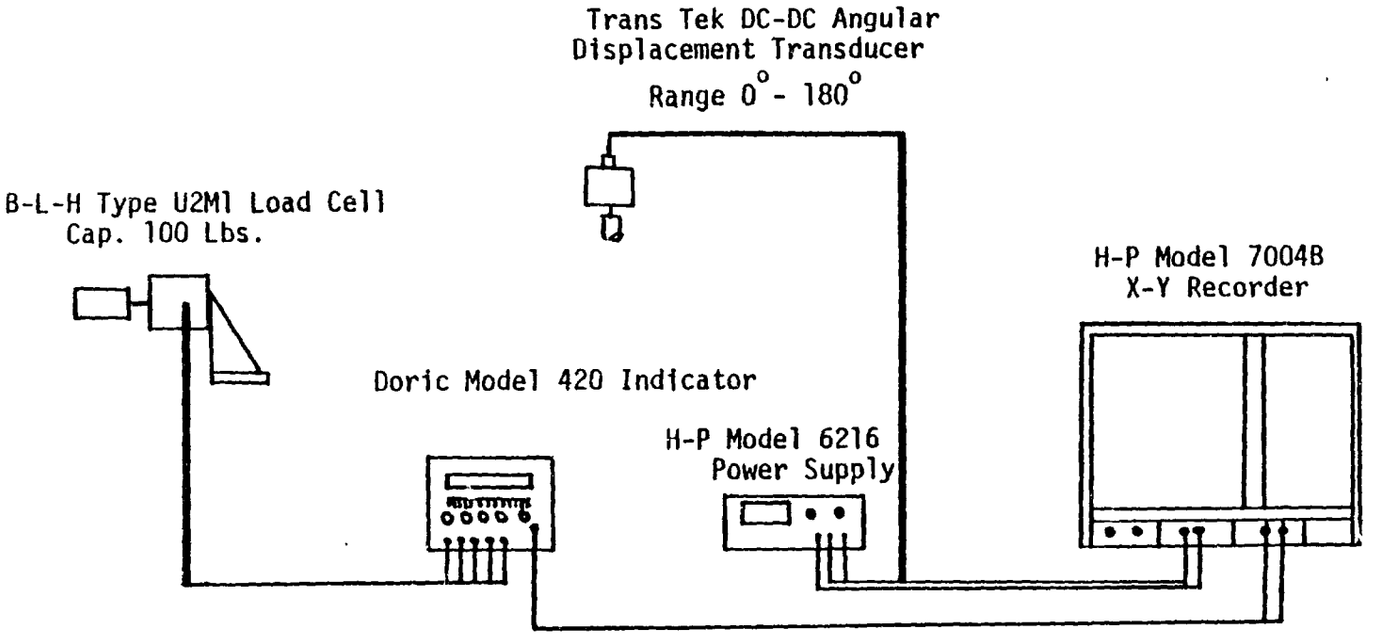

Fig. 5.2 Elastic Tube Folding Machine Instrumentation

end plate. Corresponding hole patterns were drilled into the the inserts. The two end plates were fastened to the inserts by using the appropriate set of holes.

(3) Mounting in the Testing Machine

The tube was mounted into the testing machine by bolting the end plates to the back-up plates on the machine.

(4) The x-y recorder was set up and the reading on the transducer was zeroed. The specimen data was filled in on a form (Table 6.1 is a typical data sheet).

(5) Folding of Specimens was accomplished as a two-step process-collapsing and bending. First the central part of the tube was flattened by placing the clamps a few inches apart and then tightening uniformly. The tube was then bent slightly, the clamps removed, and the tube further bent around 180°. The mounting holes were located so that each tube would be mounted with the two halves parallel and in contact.

(6) With the two arms of the test machine clamped, the clutch was put on, and the speed at which the test was to be run set. The fold radius was observed and recorded.

(7) With the pen on the x-y recorder set, the clamp on the arms was removed and the drive motor put on. During unfolding, the x-y recorder plotted the force transducer voltage versus angle transducer voltage. Voltages were shown on the indicator. Using the calibration relationship of 0.5 mv equivalent to 4.37 lbs., the force voltage was converted into pounds, then multiplied by the moment arm, 24 in., to obtain the moment. Voltage was similarly

TABLE 6.1

TEST DATA RECORDING SHEET

FOR DEPLOYMENT TESTS

SPECIMEN NO. A-79-10

DATE 11/17/79 TIME 4:30 P.M.

Angular Velocity (Deg/sec)	Force Vltg. mv	Angle Vltg mv	Moment in-lbs.	Angle Degs.	Force Vltg. mv	Angle Vltg. V	Moment in-lbs.	Angle Degs.
	$V_f(-)$	V_a	M	θ	$V_f(-)$	V_a	M	θ
	0.260	0.0	54.54	0	0.125	8.1	26.22	162
	0.210	1.0	44.05	20	0.145	8.2	30.42	164
	0.175	2.0	36.71	40	0.165	8.3	24.61	166
	0.138	3.0	28.95	60	0.213	8.4	44.68	168
	0.105	4.0	22.03	80	0.340	8.5	71.32	170
	0.090	5.0	18.88	100	0.375	8.6	78.66	172
	0.075	5.0	15.73	120	0.625	8.7	131.88	174
	0.065	7.0	13.63	140	0.500	8.8	104.88	176
	0.085	7.5	17.83	150	0.360	8.9	75.51	178
	0.095	8.0	19.93	160	0.225	9.0	47.20	180
Mean (in.) old Radius	1.55 in.							
Comments:	The specimen did snap out completely. Cracks started developing along collapsed area.							

converted to degrees on the angle scale.

Typical computations are shown in Table 6.1. M-θ relationships were plotted from this data.

(8) The strain energy was obtained from direct measurement of the areas under the curves.

On the average, each specimen was tested three times.

7. TEST RESULTS

7.1 Mechanical Properties of Material

Standard tensile coupons were cut from sheets of the 17-7PH material that had been subjected to the heat-treatment along with the test specimens. These were tested and the results are given in Table 7.1 As shown, the yield strengths averaged 179,500 and 189,500 psi in the direction of roll and transverse direction respectively.

The yield strength in the roll direction was a little below the supplier's specified value of 185,000 psi (See Table 2.1), but according to a rough stress analysis the strengths were expected to be satisfactory. As it turned out, there were buckling problems with the deployment of the tubes, but in all cases they remained elastic. This is elaborated on later.

7.2 Fabricated Specimen Shapes

The average cross-sectional properties as measured directly from the specimens are shown in Table 7.3. A comparison with the design values of R and f shows disparities which are wide in some cases. Essentially, the tubes all came out to be flatter than designed. There were contributing factors here that have been mentioned earlier. First, the forming process, as applied here, was somewhat imprecise and yielded shells that were in some cases about 10% flatter than designed. Later, the handling of the shells by the vendor during welding flattened them

TABLE 7.1

A TABULATION OF RESULTS ACQUIRED FROM TESTING

HEAT TREATED ARMCO 17-7PH SHEETS

Specimen Number	Area Sq.in.	Yield Pounds	Yield Strength P.S.I.	Tensile Strength (Pounds)	Tensile Strength (P.S.I.)
1A	0.00476	782	164,286	917	192,647
2A	0.00478	778	162,762	885	185,146
3A	0.00487	860	176,591	915	187,885
4A	0.00488	868	177,869	914	187,295
5A	0.00490	895	182,653	909	185,510
7A	0.00491	906	184,521	920	187,373
8A	0.00491	888	180,855	920	187,373
9A	0.00491	882	179,633	917	186,762
AVERAGE			176,483		
1B	0.00481	930	190,965	945	194,095
2B	0.00490	925	188,776	944	192,653
3B	0.00491	927	188,798	946	192,688
AVERAGE			189,513		

A = In the Direction of Roll

B = Transverse to Direction of Roll

TABLE 7.2

SUMMARY OF TEST DATA

Specimen	Test #	Angular Vel. Deg/sec	Mean Fold Radius (in.)	Comments
A-79-10	4	1.25	1.55	Snapped out. Cracks began to develop around collapsed area.
	5	2.0	1.55	
B-79-6	1	0.75	0.75	Specimen did not snap out. Crease pattern has a 'C'-Shaped appearance.
	2	1.25	0.75	
	3	2.50	0.75	
F-79-1	1	1.25	1.30	Specimen did not snap out. Crease pattern has a 'C'-Shaped appearance.
	2	2.00	1.30	
	3	2.50	1.30	
G-79-5	1	1.25	0.6	Specimen did not snap out. Crease pattern has a 'C'-Shaped appearance.
	2	2.00	0.6	
	3	2.50	0.6	
L-79-1	1	0.75	1.35	Specimen did not snap out. Crease pattern has a 'C'-Shaped appearance.
	2	1.25	1.35	
	3	2.50	1.35	
L-79-2	1	1.25	2.6	Specimen snapped out. Creases developed around collapsed area.
	2	1.25	2.6	
M-79-3	1	0.25	1.9	Specimen did not snap out. Crease pattern has a 'C'-Shaped appearance.
	2	1.25	1.9	
	4	2.50	1.9	

TABLE 7.3

COMPOSITE RESULTS SHEET

FOR

DEPLOYMENT TESTS

Specimen	Average Cross-sectional Properties		Test #	Strain Energy Released (lb-in)
	R_1 (in.)	f		
A-79-10	1.61	0.42	4	96.06
			5	101.73
B-79-6	1.68	0.46	1	82.38
			2	104.78
			3	105.36
F-79-1	2.22	0.40	1	87.74
			2	103.38
			3	77.10
G-79-5	3.18	0.78	1	73.56
			2	55.85
			3	66.46
L-79-1	4.40	0.75	1	88.97
			2	92.21
			3	109.19
L-79-2	4.13	0.78	1	85.34
			2	95.84
M-79-3	4.02	0.80	1	117.23
			2	116.62
			4	112.06

a little more, and finally there was some relaxation during the heat-treatment process. This disparity is not felt to seriously detract from the utility of this study since the ranges of radii and flatness resulting from the order-of-magnitude exercise performed in section 3 ($1.5 < R < 3.0$ and $0 < f < 0.67$) were not far off the range actually obtained ($1.6 < R < 4.1$ and $0.4 < f < 0.8$). Thus, the theoretical shapes were used as benchmarks, and the fabricated specimens were given designations according to their parent theoretical shape.

7.3 Deployment of Tubes

The results of the tests on seven specimens (six different shapes) are summarized in Table 7.2. As shown, the specimens were tested an average of three times each at different angular velocities. In every case the tube folded as compactly as possible with the two halves parallel and in contact. The fold radii recorded are shown.

The remarkable finding of the test series was that only two of the seven specimens deployed fully. The notation "specimen did not snap out" entered by the experimenter in the "Comments" column of Table 7.2 refers to the fact that the specimen came to rest (in self-equilibrium) in some bent position and that the center region, which had been flattened earlier, did not snap through to its original shape but instead got hung up in a buckled configuration. The tubes, however, remained elastic and could be pushed back out to their original shapes by the experimenter, and re-tested. There were, however, small wrinkles after the first test. The same behavior repeated itself on these five tubes in subsequent tests.

The only tube which both deployed fully, and remained sound structurally, was L-79-2, one of the flattest ($f = 0.78$). The remaining

tube, A-79-10, one of the rounder ones (f = 0.42), exhibited a different behavior. It failed to deploy at first, but later deployed completely, but by this time the material in the center region showed cracks.

Our major conclusion from this series of tests was that generally, this type of tube is subject to settle into a slightly bent position with the compression side of the center region attempting, but not succeeding, in expanding to its original configuration.

In researching previous experimentation with this type of tube used as a foldable member, the authors found only two previous studies; those mentioned in section 1. In the first test, conducted at NASA Lewis Research Center in 1965, (ref. 1), two tube shapes were fabricated and tested. They were both flat (f = 0.75, 0.86) and they achieved complete deployment successfully. Following up on this work in a study made for ESRO and reported in 1973 (ref. 3), one tube shape, also quite flat (f = 0.78) was fabricated and tested. It was reported and illustrated there that this phenomenon of the buckled stable configuration existed. This fault with the BFET was also reported in ref. 6. Results of the present study with flat and moderate tubes ($0.4 < f < 0.8$) are consistent with those of the ESRO study. Other instances where this tube has been utilized, to our knowledge, have been as a reelable boom where it was not required to recover from a very sharp fold.

7.4 Moment-Angle (M-θ) Curves

A comprehensive analysis of these curves is not possible due to the fact of the incomplete deployment in most cases. However, some typical curves are shown in Figs. 7-1 to 7-6, which were excerpted from ref. 7.

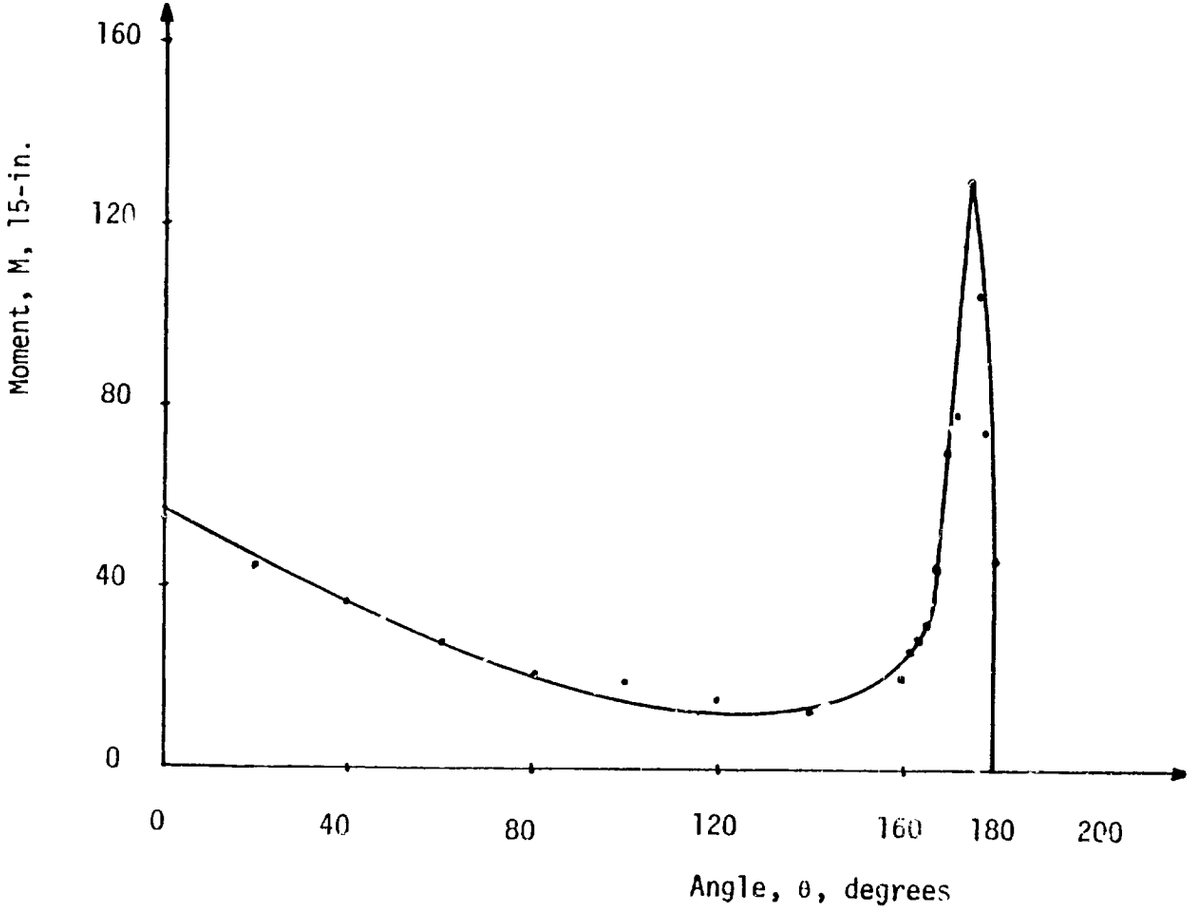

Fig. 7.1 Plot of Bending Moment in lb-in. versus Angle in degrees during deployment of A-79-10. Test #4.

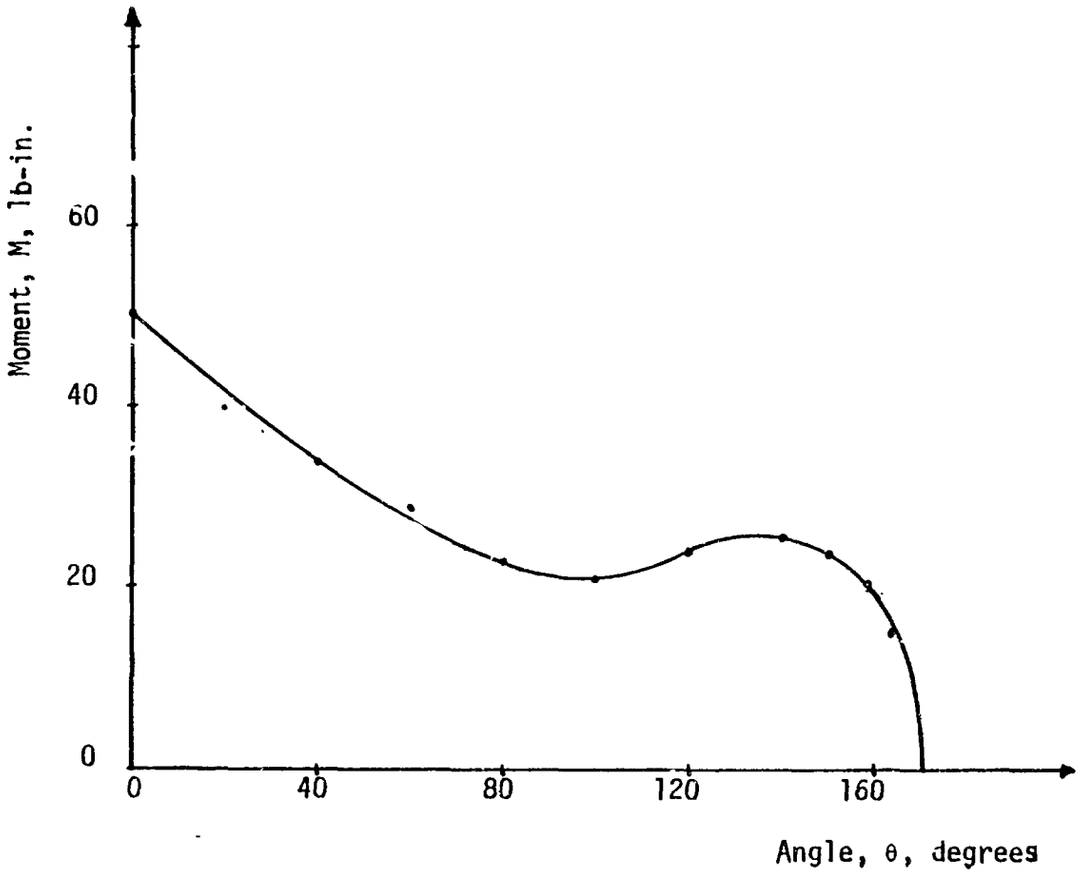

Fig. 7.2 Plot of Bending Moment in lb-in. versus Angle in degrees during deployment of B-79-6. Test #1.

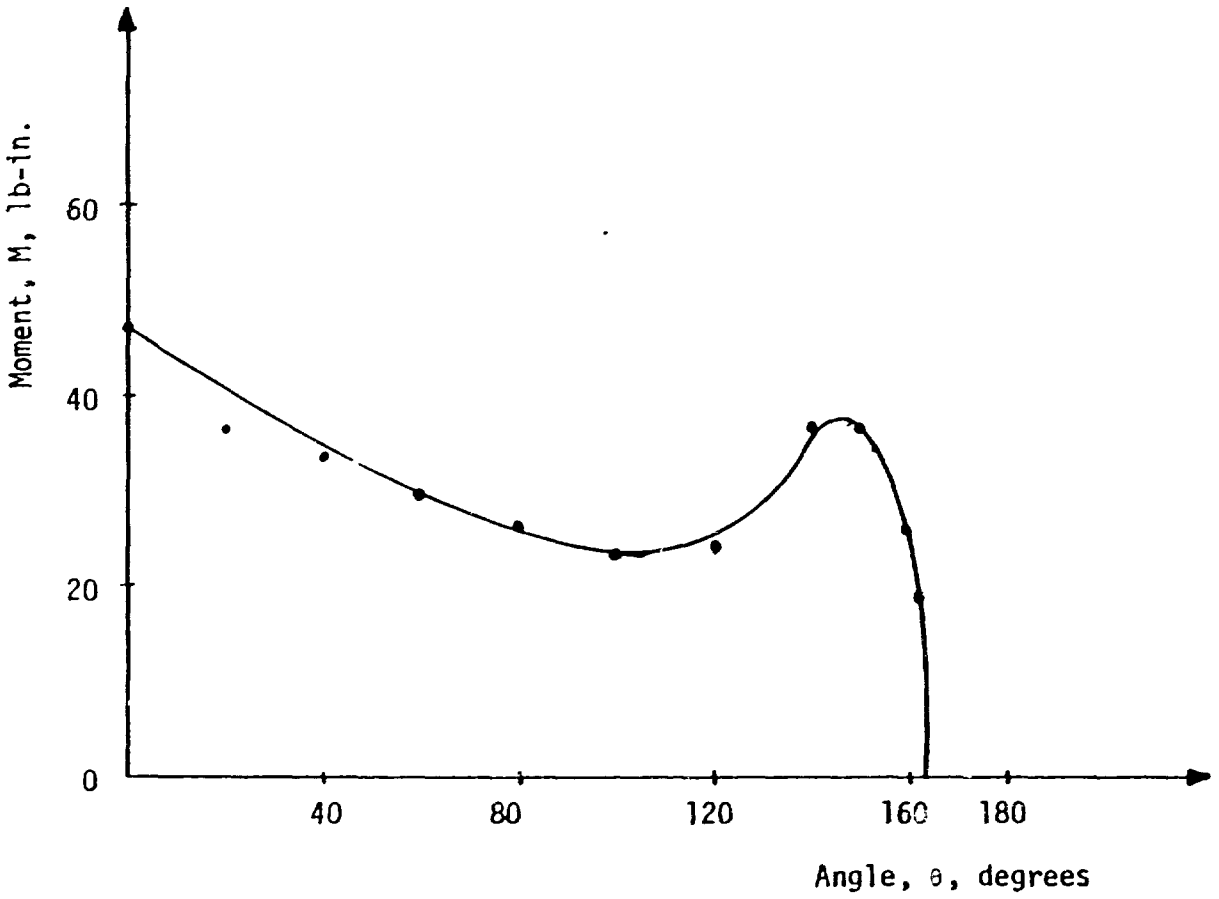

Fig. 7.3 Plot of Bending Moment in lb-in. versus Angle in degrees during deployment of F-79-1. Test #1.

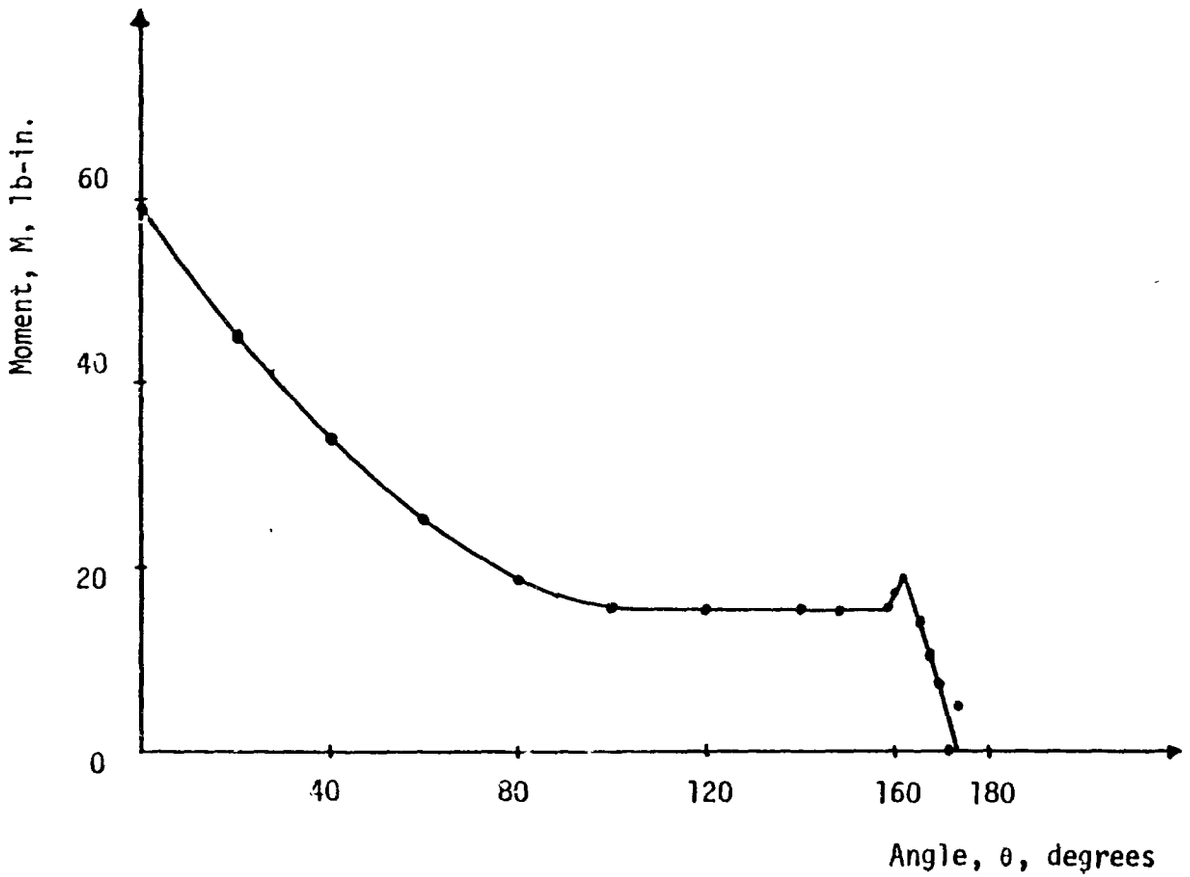

Fig. 7.4 Plot of Bending Moment in lb-in. versus Angle in degrees during deployment of G-79-5. Test #1.

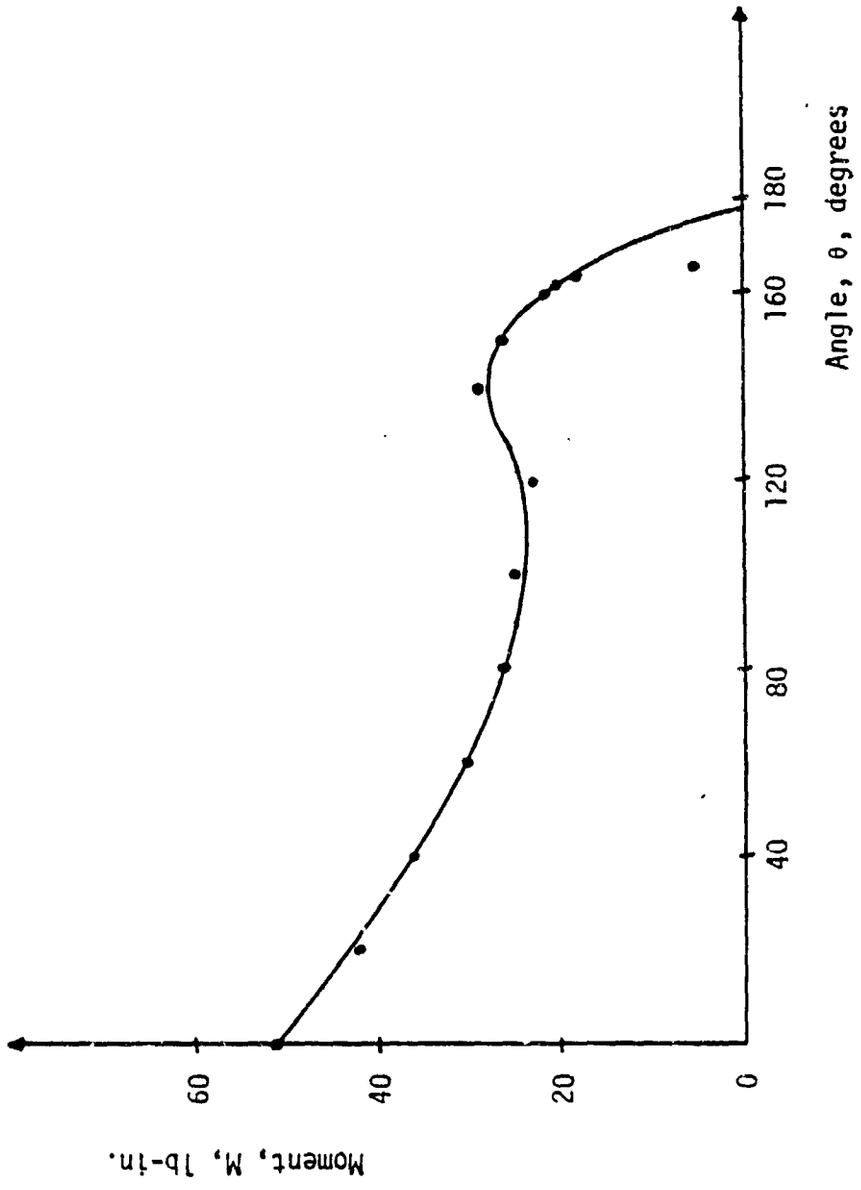

Fig. 7.5 Plot of Bending Moment in lb-in. versus Angle in degrees during deployment of L-79-1. Test #1.

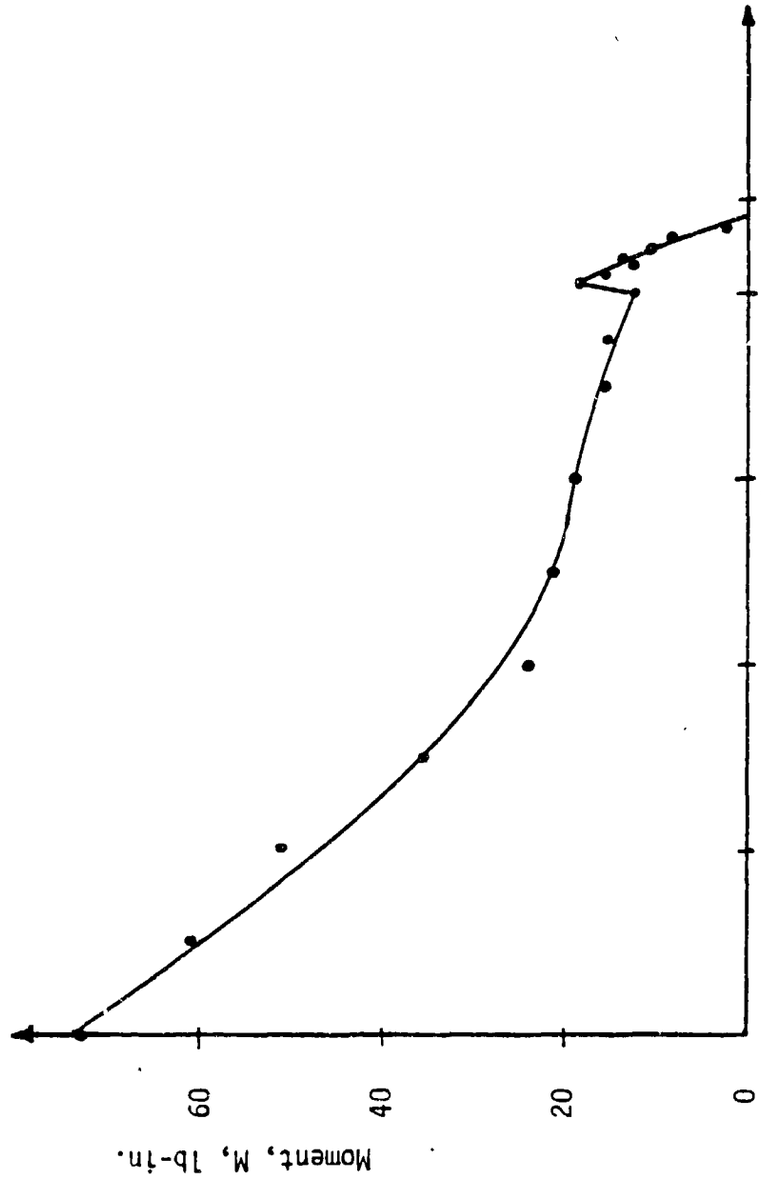

Fig. 7.6 Plot of Bending Moment in lb-in. versus Angle in degrees during deployment of L-79-2. Test #2.

Figure 7-1 is the curve for one of the tubes that fully deployed and has the characteristic, or expected, shape. The initial moment (at 0°) is about 85% of the moment that would result from taking as separate flat sheets, the upper and lower halves of the tube and bending them to the measured fold radius (1.55 in.). From this value it declines almost linearly as expected, since the central section is still flat, then rises sharply to a peak as the center region snaps outward and finally goes to zero sharply. The rise, coinciding with the opening of the central region, begins about 30% from full deployment. It has already been stated, however, that this tube had developed cracks in the central region when this curve was plotted. This point is returned to later.

The other tube which fully deployed (Fig. 7.6) did not release very much energy as its center section expanded, making its behavior similar to a linear spring. Compared to the previous (Fig. 7.1) it was considerably flatter.

The curves for the other specimens, those which did not deploy fully, are all similar. Typical ones are shown in Figs. 7-2 through 7-5. In each instance, the curves start out similar to the previous two until the point is reached when the center section is going into buckled shape. All of its energy is released then, as indicated by the hump in these curves, and the tube reaches equilibrium somewhere short of 180°; the absence of a peak indicating that there was no snap-through.

7.5 Strain Energy

Prior to the conduct of the first series of tests just described, preparations were made for analysis of the data. Specifically, it was sought to formulate an expression that would relate the strain energy released to the cross-section parameters, R and f, by statistical analysis of the test results. This work is detailed in ref.7. A functional form was assumed based upon the expectation that the energy would increase in some manner as R and decrease in some manner as f. An expression with the product of these quantities each raised to an unknown power formed the basis for a multiple regression analysis. Obviously, due to the buckling problem, most of the values of strain energy calculated from the M-θ curves are not entirely accurate. Nevertheless, to examine trends, these values were operated upon in a computer program utilized in conjunction with an IBM statistical analysis package to produce a functional relationship between strain energy and cross-section.

The strain energy calculated is shown in Table 7.3, and various curves derived from the calculated formula are shown in Figs. 7-7, 8 and 9.

7.6 Remedies for the Buckling Problem

It appeared that constraint around the center region of the tube on the compression side was impeding its snap-through. It seemed that one way to relieve some of this constraint in the lateral direction would be cut one or more slits in the tube in the longitudinal direction, on the compression side and only in the folding region. This was done

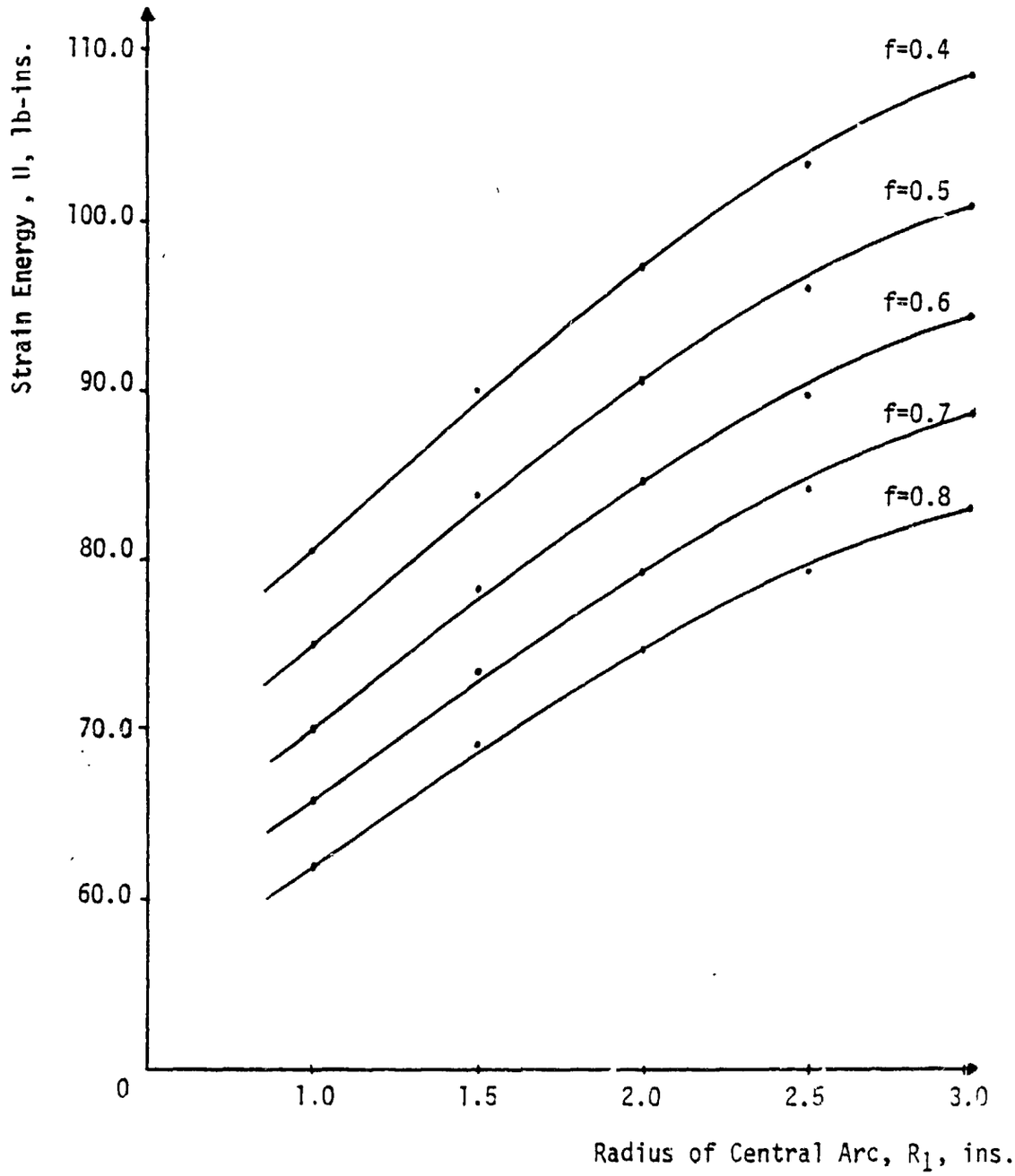

Fig. 7.7 Plot of Strain Energy in (lb-ins) versus Radius of Central Arc in (ins.) for different values of the Flatness Parameter.

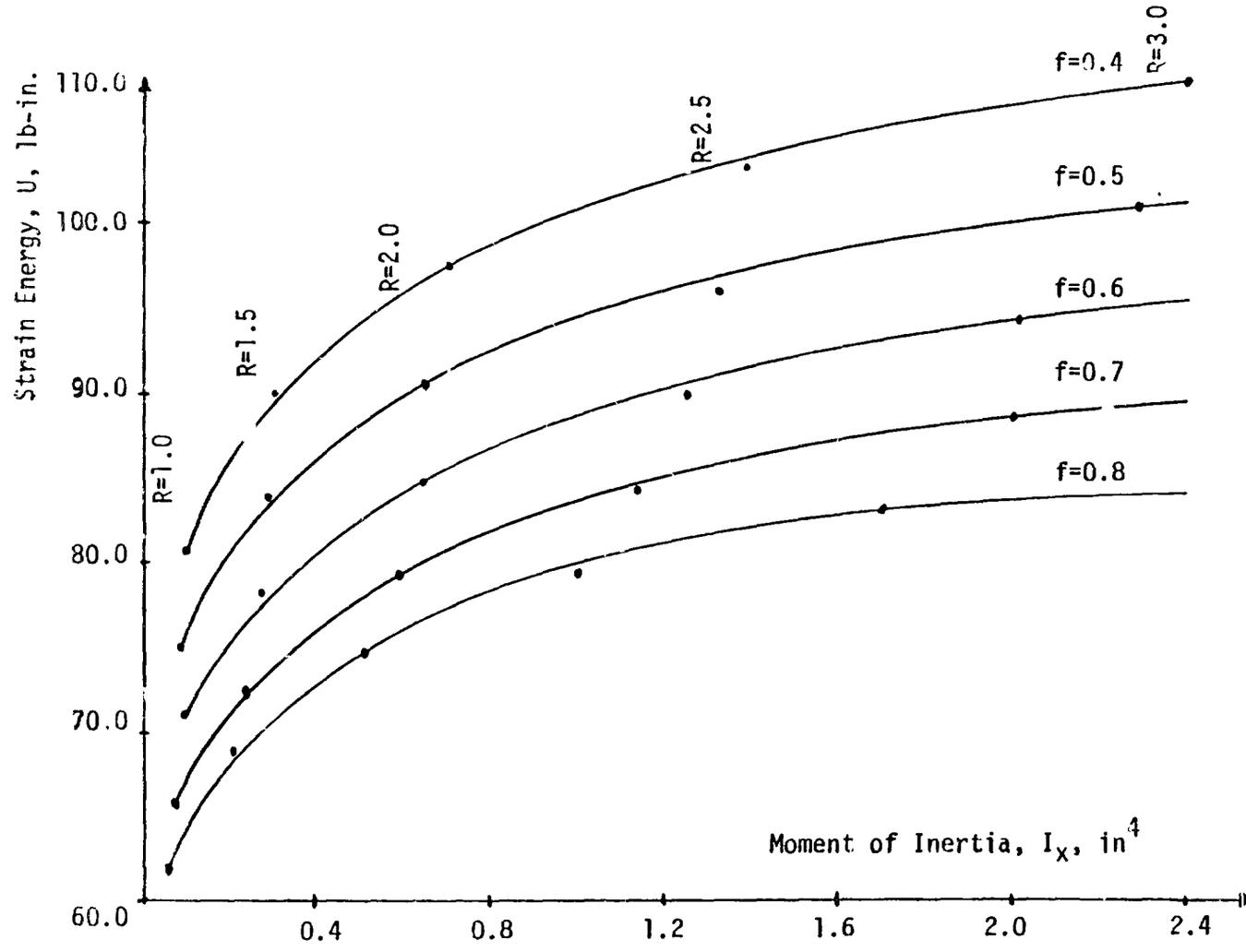

Fig. 7.8 Plot of Strain Energy in lb-in. versus Moment of Inertia I_x in (in^4) for different values of the flatness parameter.

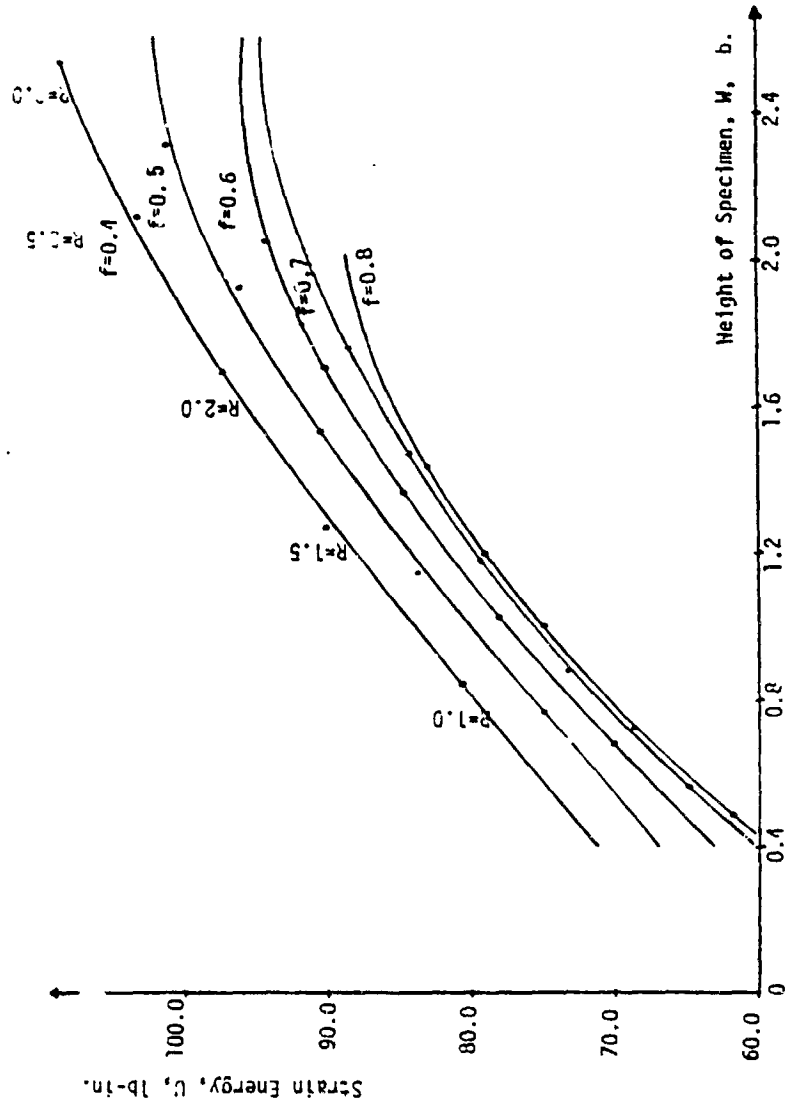

Fig. 7.9 Plot of Strain Energy in (lb-ins.) versus Height of Specimen in (lbs) for different values of the Flatness Parameter.

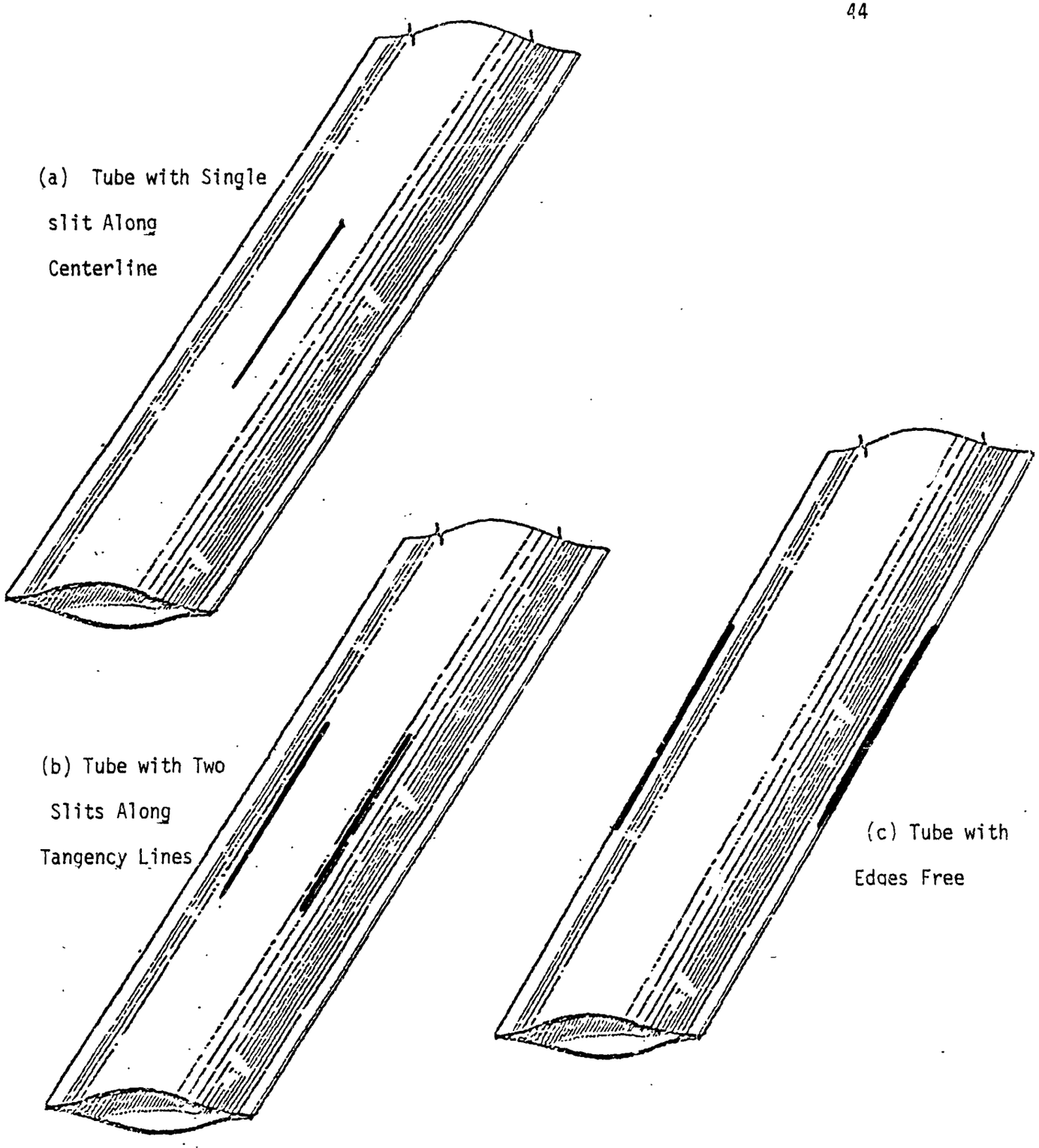

Fig. 7.14 Modified BFET's

recently on two specimens as shown in Fig. 7-14. It was decided to cut one slit in the center of a flat specimen (G-79-2, f = 0.70), and two symmetrical slits in a rounder specimen (F-79-3), f = 0.40). In both cases, these tubes, which previously settled into buckled equilibrium, now deployed fully every time tested. While the slits relieved the buckling problem, it would appear that they would slightly reduce the energy released and local buckling strength. These characteristics will be investigated in the future.

Other strain relieving techniques will be attempted by the authors in an effort to optimize the design of this tube while keeping it reliably deployable.

8. CONCLUSIONS

The majority of work performed on this project in Phase I has been in preparation for conducting the first series of tests, which are reported here. These tests indicated the need for a design modification in the BFET due to its failure to deploy fully. The authors have several possible modifications in mind and have begun work on one. With the FET testing machine set-up, and shell forming apparatus in place, the authors anticipate development of this and other types of foldable tubes in the continuation of this investigation.

REFERENCES

1. Gertsma, L. W., Dunn, J. H., Kempke, E. E., Jr. : Evaluation of One Type of Foldable Tube, NASA TM X-1187, December 1965.

2. Gertsma, L. W., et al. : Foldable Conduit, U.S. Patent No. 3,295,556 January, 1967.

3. Fernandez-Sintes, J., Cristos, J.C. : Foldable Elastic Tubes for Hinges on Satellites, Contractor Report ESRO-CR 65 by Instituto Nacional de Tecnica Aerospacial, Madrid, Spain, for the European Space Research Organization.

4. Product Data, Armco 17-7PH Precipitation Hardening Stainless Steel Sheet and Strip, Armco Steel Corp. Advanced Materials Division, Baltimore, Maryland.

5. Mikulus, M. M., Bush, H. G., Card, M. F. : Structural Stiffness, Strength and Dynamic Characteristics of Large Tetrahedral Space Truss Structures, NASA TM X-74001, March 1977.

6. Crawford, R. F. : Strength and Efficiency of Deployable Booms for Space Applications, AIAA Paper No. 71-396, Variable Geometry and Expandable Structures Conference, April, 1971.

7. Boateng, C. : Deployment Tests for One Type of Foldable Elastic Tube (BFET), Master's Degree Thesis, Howard University, December, 1979.

APPENDIX A

Standard Heat Treatments for
Armco 17-7PH Stainless Steel

STANDARD HEAT TREATMENTS

Three essential steps are required in heat treating 17-7 PH to Conditions TH 1050 and RH 950:

1. Austenite Conditioning
2. Cooling to effect transformation of austenite to martensite
3. Precipitation Hardening

Following are the procedures for heat treating material in Condition A to Conditions TH 1050 and RH 950:

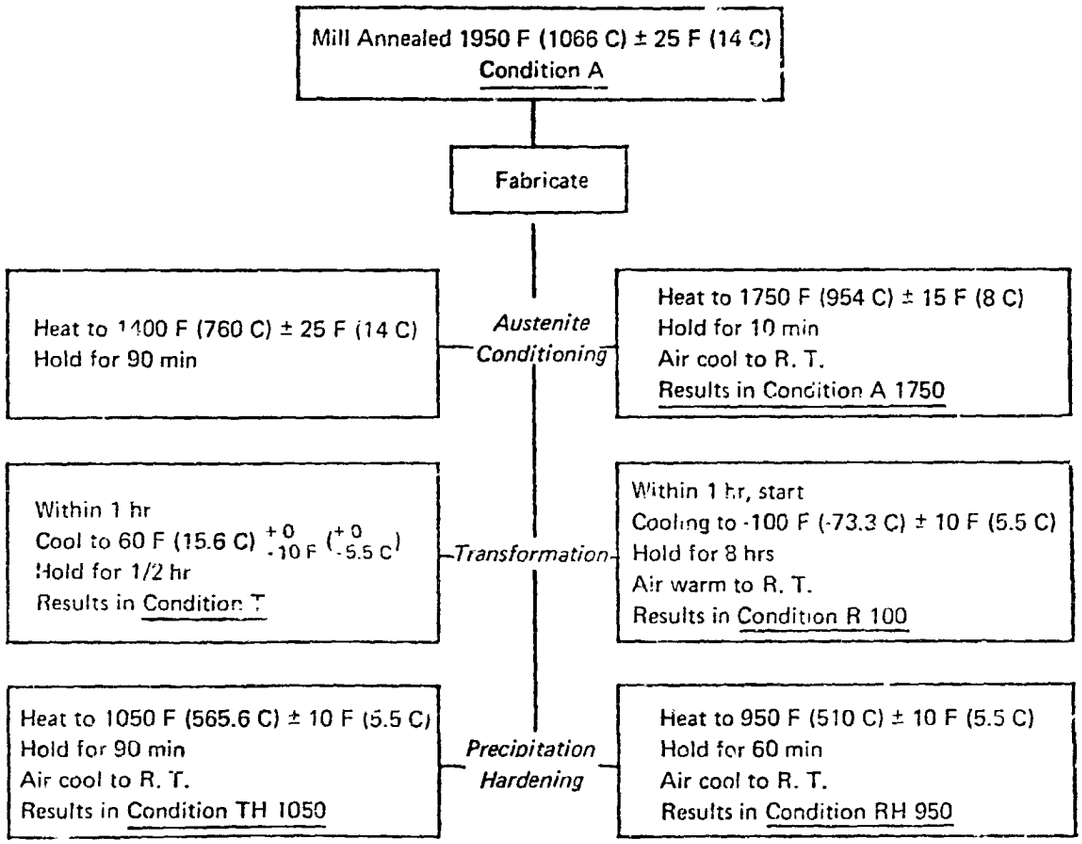

NOTE:

Full strength may not be developed when cold worked material is heat treated to Condition TH 1050. However, full strength will be developed by using one of the following methods:

1. Re-anneal the fabricated part to Condition A and heat treat to Condition TH 1050.
2. Heat treat fabricated part to an RH 1050 Condition.
3. Use a modified TH 1050 heat treatment. For further information on this heat treatment, contact Armco or your Distributor.

No variation in properties is encountered when heat treating fabricated parts to Condition RH 950.

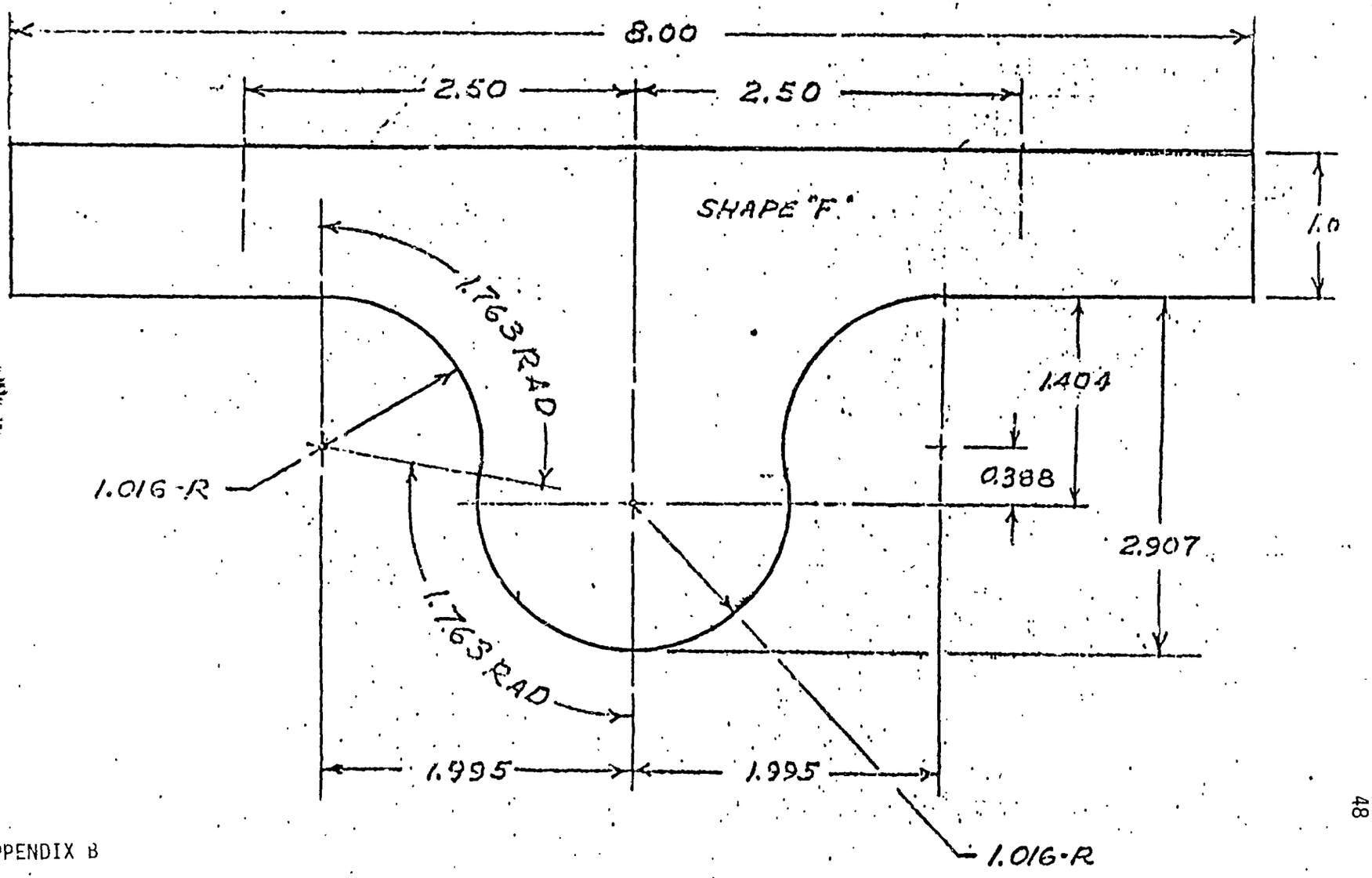

APPENDIX B

Typical Form Block Drawing

ORIGINAL PAGE IS
OF POOR QUALITY

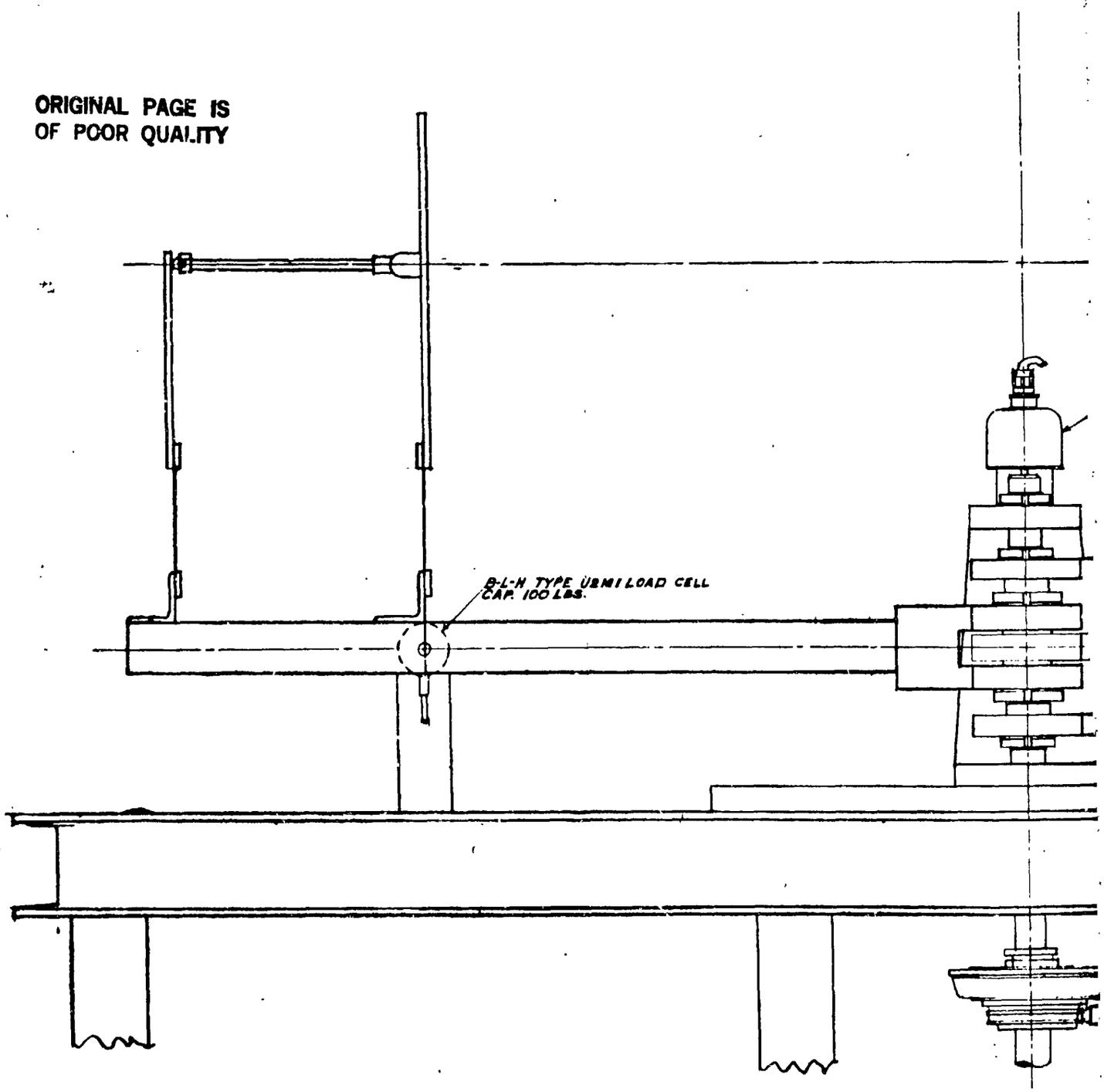

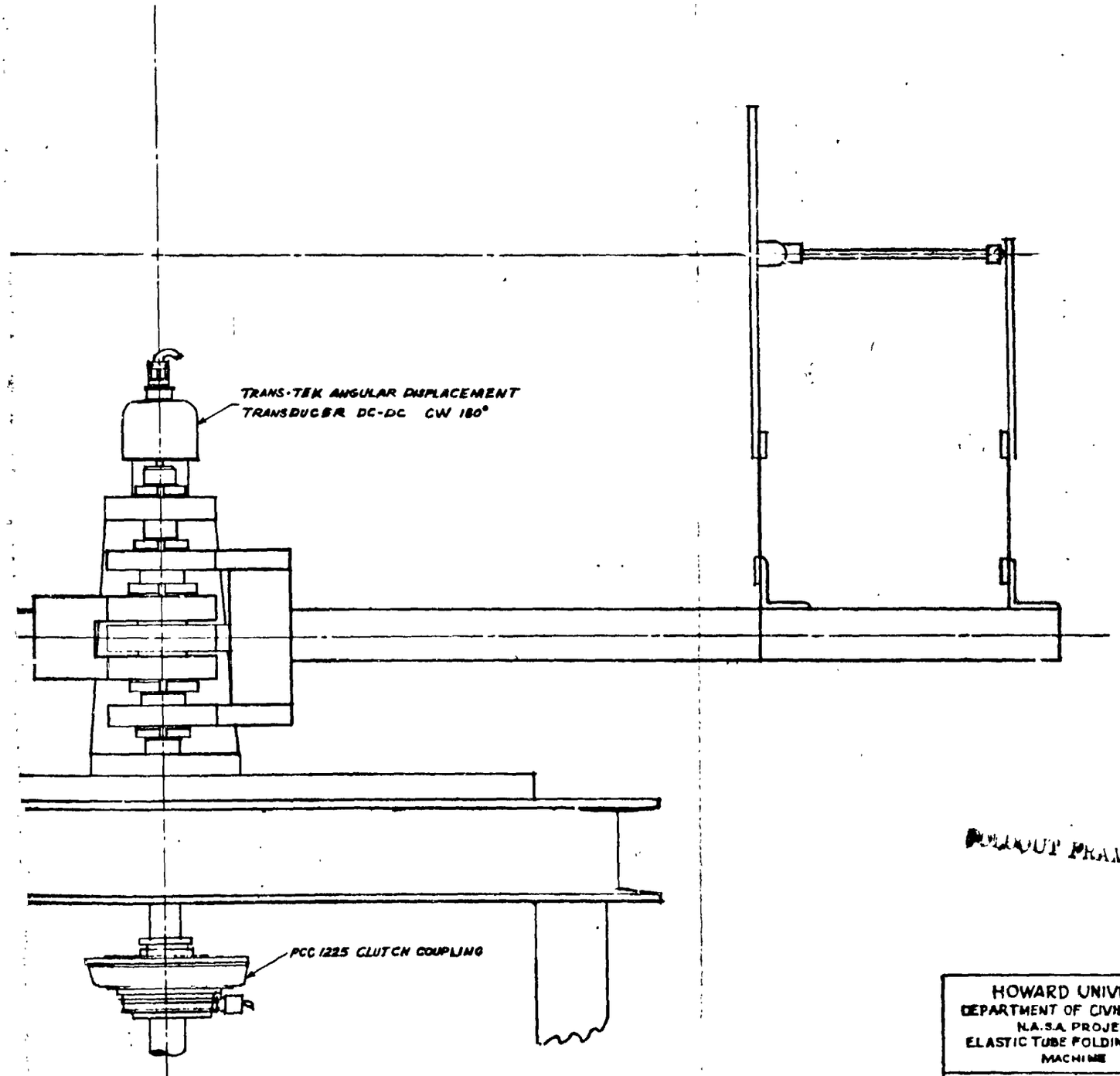

PULLOUT FRAME

HOWARD UNIVERSITY
DEPARTMENT OF CIVIL ENGINEERING
N.A.S.A. PROJECT
ELASTIC TUBE FOLDING TESTING
MACHINE

MACHINE ASS'Y

DESIGNED BY:	DRAWN BY:	
CHECK'D BY:	SCALE: 1" = 1'	PART NO.
REVS	DATE 1-24-79	PAGE 1 OF 1

APPENDIX C

Assembly Drawing- FET Testing Mach